Mutual Inductance in Wave Filters with an Introduction on Filter Design

By K. S. JOHNSON and T. E. SHEA

PART I

General Principles of Wave Filter Design

Principles of Generalized Dissymmetrical Networks. We shall consider first the impedance and propagation characteristics of certain generalized networks. It can be shown that *any passive network having one pair of input and one pair of output terminals may, at any frequency, be completely and adequately represented by an equivalent T or π net-*

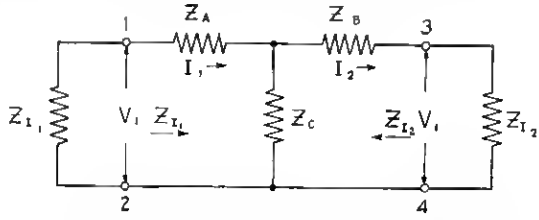

Fig. 1—Generalized Dissymmetrical T Network Connected to Impedances Equal to Its Image Impedances

work.[1] The impedance and propagation characteristics of any such network may be expressed in terms of its equivalent T or π network. These characteristics are defined by (1) the *image impedances*, and (2) the *transfer constant*, the latter including the *attenuation constant*[2] and the *phase constant.*[2] In the case of a symmetrical network, the image impedances and the transfer constant are, respectively, the *iterative impedances* (or *characteristic impedances*) and the *propagation constant* employed by Campbell, Zobel, and others. The terms involved will be subsequently defined.

Consider the dissymmetrical T network of Fig. 1. If the 3−4 terminals of the T network are connected to an impedance Z_{I_2}, the

[1] Campbell, G. A., "Cisoidal Oscillations," *Transactions A. I. E. E.*, (1911), Vol. XXX, Part II, pp. 873-909.

The T and π networks referred to above are sometimes called *star* (Y) and *delta* (Δ) networks, respectively.

[2] The real and imaginary parts of the transfer constant have been called by Zobel, the *diminution constant* and the *angular constant*, respectively. (See Bibliography 13.)

impedance looking into the T network at the $1-2$ terminals will be

$$Z_{1-2}=Z_A+\frac{Z_C(Z_B+Z_{I_2})}{Z_C+Z_B+Z_{I_2}}. \tag{1}$$

Similarly, if the $1-2$ terminals of the T network are connected to an impedance Z_{I_1}, the impedance looking into the $3-4$ terminals of the T network will be

$$Z_{3-4}=Z_B+\frac{Z_C(Z_A+Z_{I_1})}{Z_C+Z_A+Z_{I_1}}. \tag{2}$$

If Z_{1-2} is equal to the terminal impedance Z_{I_1}, and if, similarly, Z_{3-4} is equal to the terminal impedance Z_{I_2}, the network will then be terminated in such a way that, at either junction ($1-2$ or $3-4$), the impedance in the two directions is the same. In other words, at each junction point, the impedance looking in one direction is the *image* of the impedance looking in the opposite direction. Under these conditions Z_{I_1} and Z_{I_2} are called the *image impedances* of the T network. If equations (1) and (2) are solved explicitly for Z_{I_1} and Z_{I_2}, the following expressions are obtained:

$$Z_{I_1}=\sqrt{\frac{(Z_A+Z_C)(Z_AZ_B+Z_AZ_C+Z_BZ_C)}{(Z_B+Z_C)}}, \tag{3}$$

$$Z_{I_2}=\sqrt{\frac{(Z_B+Z_C)(Z_AZ_B+Z_AZ_C+Z_BZ_C)}{(Z_A+Z_C)}}. \tag{4}$$

If Z_{oc} is the impedance looking into one end of the network with the distant end open-circuited, and if Z_{sc} is the corresponding impedance with the distant end short-circuited, it may be shown that the image impedance at either end of the network is the geometric mean of Z_{oc} and Z_{sc}. What is here termed the image impedance is, therefore, equivalent to what Kennelly has called the *surge impedance.*[3]

The propagation characteristics of a dissymmetrical network may be completely expressed in terms of the transfer constant. The transfer constant of any structure may be defined as one-half the natural logarithm of the vector ratio of the steady-state vector volt-amperes entering and leaving the network when the latter is terminated in its image impedances. The ratio is determined by dividing the value of the vector volt-amperes at the transmitting end of the network by the value of the vector volt-amperes at the receiving end.

[3] There is at present lack of common agreement as to the basis of definition of this term, and it is often defined upon the basis, not of open and short-circuit impedances, but of a uniform recurrent line (See A. I. E. E. Standardization Rule 12054, edition of 1922). The formulae derived by the two methods are not equivament in the case of dissymmetrical networks.

The real part of the transfer constant, that is, the *attenuation constant*, is expressed by the above definition in *napiers* or *hyperbolic radians* and the imaginary part, that is, the *phase constant*, is expressed in circular *radians*. The practical unit of attenuation here

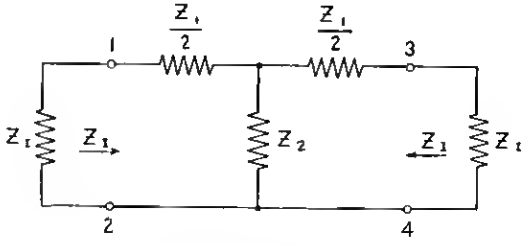

Fig. 2—Generalized Symmetrical T Network Connected to Impedances Equal to Its Image Impedances

used is the *transmission unit*[4] (1 TU=.11513 napier). It can be demonstrated that the transfer constant, Θ, of the T network shown in Fig. 1 is

$$\Theta=\tanh^{-1}\sqrt{\frac{Z_{sc}}{Z_{oc}}}=\tanh^{-1}\sqrt{\frac{Z_AZ_B+Z_AZ_C+Z_BZ_C}{(Z_A+Z_C)(Z_B+Z_C)}}$$
$$=\cosh^{-1}\sqrt{\frac{(Z_A+Z_C)(Z_B+Z_C)}{Z_C^2}}, \tag{5}$$

in which Z_{oc} and Z_{sc} are, as previously defined, the open and short-circuit impedances of the network. The ratio Z_{sc}/Z_{oc} is the same at both ends of any passive network.

Principles of Generalized Symmetrical Networks. Consider now the impedance and propagation characteristics of the generalized symmetrical structure shown in Fig. 2. On account of the symmetry of the structure, the image impedances at both ends are identical, and from equation (3) or (4) their value may be shown[5] to be

$$Z_I=\sqrt{Z_1Z_2\left(1+\frac{Z_1}{4Z_2}\right)}. \tag{6}$$

In the case of a symmetrical T structure, such as is shown in Fig. 2, the impedance Z_I is called the *mid-series image impedance.* The significance of this term will be evident, if the series-shunt type of

[4] W. H. Martin, "The Transmission Unit and Telephone Transmission Reference System," *Bell Sys. Tech. Jour.*, July, 1924; *Jour. A. I. E. E.*, Vol. 43, p. 504, 1924.

[5] Zobel, O. J., "Theory and Design of Uniform and Composite Electric Wave-Filters," *Bell Syst. Tech. Jour.*, Jan., 1923.

structure shown in Fig. 3 is regarded as made up of symmetrical T networks or sections, the junctions of which occur at the mid-points of the series arms.

Suppose now that the structure of Fig. 3 is considered to be made up of symmetrical π networks, or sections, each of which is represented

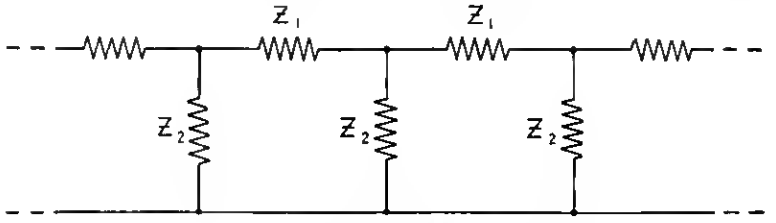

Fig. 3—Generalized Recurrent Series-Shunt Network

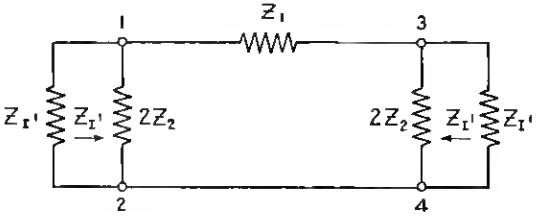

Fig. 4—Generalized Symmetrical π Network Connected to Impedances Equal to Its Image Impedances

as in Fig. 4. By methods similar to those employed for the T network of Fig. 2 it can be shown[5] that the image impedance of the generalized π network of Fig. 4 is given by

$$Z_{I'} = \sqrt{\frac{Z_1 Z_2}{1+\frac{Z_1}{4Z_2}}}. \tag{7}$$

In this symmetrical structure the image impedance is called the *mid-shunt image impedance.*

The image transfer constant of either a T or a π symmetrical structure is[5]

$$\Theta = A + jB = 2\ \sinh^{-1}\sqrt{\frac{Z_1}{4Z_2}} = \cosh^{-1}\left(1+\frac{Z_1}{2Z_2}\right). \tag{8}$$

In discussing the generalized networks of Figs. 1, 2 and 4, it has been assumed that the networks were terminated in their respective image impedances. In practical cases, filters must be designed to work between impedances which are, in general, not exactly equal to their

image impedances at more than one or a few frequencies. For a generalized structure, such as that of Fig. 1, operating between a *sending-end impedance* Z_S and a *receiving-end impedance* Z_R, the current in Z_R, for an electromotive force acting in Z_S, is

$$I_R = \frac{E}{Z_S+Z_R} \times \frac{Z_S+Z_R}{\sqrt{4Z_SZ_R}} \times \frac{\sqrt{4Z_{I_1}Z_S}}{Z_{I_1}+Z_S} \times \frac{\sqrt{4Z_{I_2}Z_R}}{Z_{I_2}+Z_R} \times \epsilon^{-\theta} \times \frac{1}{1-\frac{Z_{I_2}-Z_R}{Z_{I_2}+Z_R} \times \frac{Z_{I_1}-Z_S}{Z_{I_1}+Z_S} \times \epsilon^{-2\theta}}. \tag{9}$$

Since $E/(Z_S+Z_R)$ is the current ($I_{R'}$) which would flow if the generalized T network were not inserted in the circuit, the ratio of the received current, *with* and *without* the network in the circuit, may be expressed by the relation

$$\frac{I_R}{I_{R'}} = \left(\frac{Z_S+Z_R}{\sqrt{4Z_SZ_R}}\right)\left(\frac{\sqrt{4Z_{I_1}Z_S}}{Z_{I_1}+Z_S}\right)\left(\frac{\sqrt{4Z_{I_2}Z_R}}{Z_{I_2}+Z_R}\right) \times \epsilon^{-\theta} \times \frac{1}{1-\left(\frac{Z_{I_2}-Z_R}{Z_{I_2}+Z_R}\right)\left(\frac{Z_{I_1}-Z_S}{Z_{I_1}+Z_S}\right)\epsilon^{-2\theta}}. \tag{10}$$

In general, the electromotive force does not act through a simple sending-end impedance Z_S but through some complex circuit. The current ratio ($I_R/I_{R'}$) will, however, be the same in either case. The principle underlying this fact is known as *Thévenin's Theorem*.[6]

The absolute magnitude of the current ratio, $\left|I_R/I_{R'}\right|$, is a measure of the *transmission loss* caused by the introduction of the network. The transmission loss may be expressed in terms of transmission units (TU) by aid of the following relation

$$TU = 20 \log_{10}\left|\frac{I_{R'}}{I_R}\right|. \tag{11}$$

Reference to equation (10) shows that the transmission loss caused by the introduction of any network is composed of five factors. The first three factors of this equation are all of the same general type with the exception that the first of the three is reciprocal in nature to the other two. These two latter factors have been called *reflection factors* and determine the *reflection losses* which exist between the impedances involved. The fourth factor is the *transfer factor* and expresses the current ratio which corresponds to the transfer con-

[6] Casper, W. L., "Telephone Transformers," *Transactions A. I. E. E.*, March, 1924, p. 4. Thévenin, M. L., "Sur un Nouveau Théorème d'Electricité Dynamique," *Comptes Rendus*, vol. 97, p. 159, 1883.

stant. The last factor has been called the *interaction factor*. The value of the reflection factor is evidently a function simply of the *ratio* of the impedances involved, while the absolute value of the transfer factor is ϵ^{-A} where A is the real portion of the transfer constant and hence is the attenuation constant. The value of the interaction factor is seen to be unity either when $Z_{I_2}=Z_R$ or when $Z_{I_1}=Z_S$. It also approaches unity if the value of Θ is sufficiently large.

In the case of a symmetrical structure, such as is shown in Fig. 2, or Fig. 4, $Z_{I_1}=Z_{I_2}=Z_I$ and equation (10) reduces to

$$\frac{I_R}{I_{R'}}=\left(\frac{Z_S+Z_R}{\sqrt{4Z_SZ_R}}\right)\left(\frac{\sqrt{4Z_IZ_S}}{Z_I+Z_S}\right)\left(\frac{\sqrt{4Z_IZ_R}}{Z_I+Z_R}\right)\times\epsilon^{-\theta}\times\frac{1}{1-\left(\frac{Z_I-Z_R}{Z_I+Z_R}\right)\left(\frac{Z_I-Z_S}{Z_I+Z_S}\right)\epsilon^{-2\theta}}. \tag{12}$$

If the structure is symmetrical, and if, furthermore, the sending-end impedance Z_S is equal to the receiving-end impedance Z_R, equation (12) becomes

$$\frac{I_R}{I_{R'}}=\epsilon^{-\theta}\times\frac{4Z_IZ_R}{(Z_I+Z_R)^2}\times\frac{1}{1-\left(\frac{Z_I-Z_R}{Z_I+Z_R}\right)^2\epsilon^{-2\theta}}. \tag{13}$$

The preceding formulae make it possible to calculate rigorously the transmission loss caused by any network whose image impedances and transfer constant are both known. In the symmetrical case, if $Z_I=Z_S=Z_R$, the transmission loss is determined simply by the value of the attenuation constant. In general, in the attenuation range of frequencies, the value of Θ of a wave filter is relatively large and the interaction factor is substantially unity. Consequently, the transmission loss caused by any filter in its attenuation range is dependent practically only upon the value of the attenuation constant and the reflection losses between Z_S and Z_{I_1}, Z_R and Z_{I_2}, and Z_S and Z_R, respectively. Throughout most of the transmission range of a filter, its image impedances may be made very closely equal to the terminating impedances so that the transmission loss caused by the filter in this range is dependent simply upon its attenuation constant. In the intervening range, between the attenuated and the non-attenuated bands, the transfer factor, the reflection factors and the interaction factor must all be taken into account.[7]

[7] Zobel, O. J., "Transmission Characteristics of Electric Wave-Filters," *Bell Sys. Tech. Jour.*, Oct., 1924.

Impedance and Propagation Characteristics of Non-Dissipative Filters. If the series and shunt impedances of the structures shown in Figs. 2 and 4 are pure reactances, as they would be in the case of a non-dissipative filter, the ratio of the quantity $Z_1/4Z_2$ must be either a positive or negative numeric. It has been shown by Campbell[8] and others that the attenuation constant is zero, and that the structure freely transmits at all frequencies at which the ratio $Z_1/4Z_2$ lies between 0 and -1. Therefore, by plotting values of the ratio $Z_1/4Z_2$ it is possible to determine the attenuation characteristic of any symmetrical structure as a function of frequency.

In the transmission range, the phase constant of the symmetrical structure shown in Fig. 2 or Fig. 4, is

$$B = 2 \sin^{-1}\sqrt{\frac{-Z_1}{4Z_2}}. \tag{14}$$

Hence, the expression for the image transfer constant of either of the symmetrical structures shown in Fig. 2 or Fig. 4 is

$$\Theta = 0 + j\, 2 \sin^{-1}\sqrt{\frac{-Z_1}{4Z_2}}. \tag{15}$$

In the attenuation region, $Z_1/4Z_2$ may be either negative or positive. If $Z_1/4Z_2$ is negative and is greater in absolute magnitude than unity, the attenuation constant is

$$A = 2 \cosh^{-1}\sqrt{\frac{-Z_1}{4Z_2}} \tag{16}$$

and the phase constant, or the imaginary component of the image transfer constant, is

$$B = (2K-1)\pi \tag{17}$$

where K is any integer. Hence,

$$\Theta = 2 \cosh^{-1}\sqrt{\frac{-Z_1}{4Z_2}} + j(2K-1)\pi. \tag{18}$$

From equation (8), when $Z_1/4Z_2$ is positive, the attenuation constant is

$$A = 2 \sinh^{-1}\sqrt{\frac{Z_1}{4Z_2}} \tag{19}$$

and the phase constant B is zero. Hence,

$$\Theta = 2 \sinh^{-1}\sqrt{\frac{Z_1}{4Z_2}} + j0. \tag{20}$$

[8] Campbell, G. A., "Physical Theory of the Electric Wave-Filter," *Bell Sys. Tech. Jour.*, Nov., 1922.

As a result of equations (18) and (20), in the attenuation range, the phase constant of a non-dissipative symmetrical filter section is always zero or an odd multiple of $\pm\pi$.

The *cut-off frequencies*, by which are meant the divisional frequencies which separate the transmission bands from the attenuation bands, must always occur when $Z_1/4Z_2=0$ or when $Z_1/4Z_2=-1$, since, for the transmission bands, $Z_1/4Z_2$ must lie between 0 and -1.

The general formulae for the image impedances of the symmetrical networks shown in Figs. 2 and 4 are equations (6) and (7), respectively. From these equations, the image impedances are pure resistances in the transmission range of a non-dissipative structure. In the attenuation range, however, the image impedances are pure reactances; the mid-series image impedance is a reactance having the same sign as Z_1, while the mid-shunt image impedance is a reactance having the same sign as Z_2. In these attenuation bands, the image impedances (pure reactances) have positive or negative signs depending upon whether they are increasing or decreasing with frequency. The order of magnitude of the image impedances may be found from Table I.

TABLE I

If the Value of $\lvert Z_1 \rvert$ is	And if the Value of $\lvert 4Z_2 \rvert$ is	Then the Mid-Series Image Impedance is	And the Mid-Shunt Image Impedance is
Zero	Zero	Zero	Zero
Zero	Finite	Zero †	Zero †
Zero	Infinite	Finite †	Finite †
Finite	Zero	Finite **	Zero **
Finite	Finite	Zero* or Finite	Infinite * or Finite
Finite	Infinite	Infinite †	Infinite †
Infinite	Zero	Infinite **	Zero **
Infinite	Finite	Infinite **	Finite **
Infinite	Infinite	Infinite	Infinite

* When both Z_1 and Z_2 are finite and $Z_1=-4Z_2$, the mid-series image impedance is zero and the mid-shunt image impedance is infinite.

† This condition gives a cut-off frequency.

** This condition results in infinite attenuation.

Types of Non-Dissipative Series-Shunt Sections Having Not More Than One Transmission Band or More Than One Attenuation Band. Since the series and shunt arms of a non-dissipative filter section may each be composed of any combination of pure reactances, it is possible to have an infinite number of types of filter sections. However, it is seldom desirable to employ filters having more than one transmission band or more than one attenuation band. Under these conditions,

it is generally impracticable to employ more than four reactance elements in either of the arms of a section. Likewise, a total of six reactance elements in both the series and shunt arms is the maximum that can be economically employed.

Types of two-terminal reactance meshes having not more than four elements, are listed in Fig. 5. In Fig. 6, the corresponding frequency-

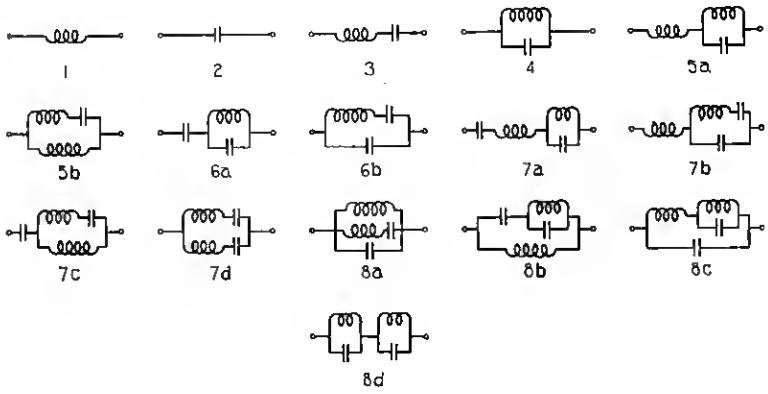

Fig. 5—Two-Terminal Reactance Meshes Containing Not More Than Four Elements

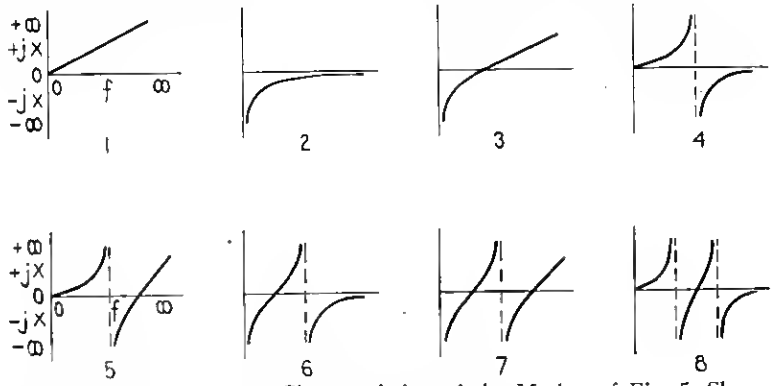

Fig. 6—Reactance-Frequency Characteristics, of the Meshes of Fig. 5, Shown in Symbolic Form

reactance characteristics are represented. Reactance characteristics Nos. 1 and 2 of Fig. 6 are reciprocal in nature, that is, their product is a constant, independent of frequency. Reactance characteristics Nos. 3 and 4 are similarly related if the frequencies of resonance and anti-resonance coincide. Similar relations exist between characteristics Nos. 5 and 6, and between characteristics Nos. 7 and 8. Two forms of reactance mesh in Fig. 5 (Nos. 5a and 5b) give the same

reactance characteristic (No. 5 of Fig. 6) and are, therefore, by proper design, electrically equivalent. Characteristic No. 6 of Fig. 6 also corresponds to two reactance meshes of Fig. 5 (Nos. 6a and 6b) and the latter may, therefore, be considered equivalent. Likewise, reactance meshes 7a, 7b, 7c and 7d of Fig. 5 give characteristic No. 7 of Fig. 6 and are therefore potentially equivalent; also reactance

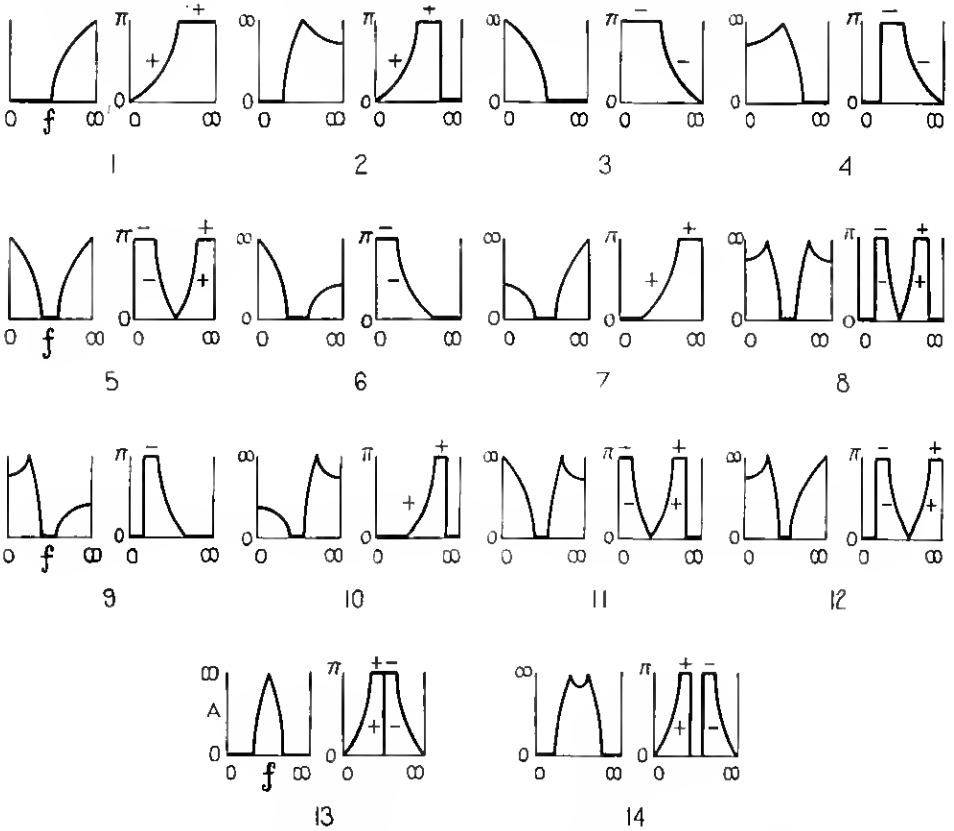

Fig. 7—Propagation Constant (Attenuation Constant and Phase Constant) Characteristics, Shown in Symbolic Form

meshes Nos. 8a, 8b, 8c and 8d of Fig. 5 are represented by reactance characteristic No. 8 of Fig. 6 and, consequently, may also be designed to be equivalent. The equivalence of the above reactance meshes has been discussed by Zobel [5] and will be subsequently treated at length. It is to be understood that, for the sake of brevity, in what follows, meshes Nos. 5, 6, 7 and 8 cover, respectively, all forms of the equivalent meshes: 5a and 5b; 6a and 6b; 7a, 7b, 7c and 7d; and

8a, 8b, 8c and 8d. Using these reactance combinations [9] for the series and shunt arms, there are only a relatively small number of types of filter structures. All of these types of filter structures are

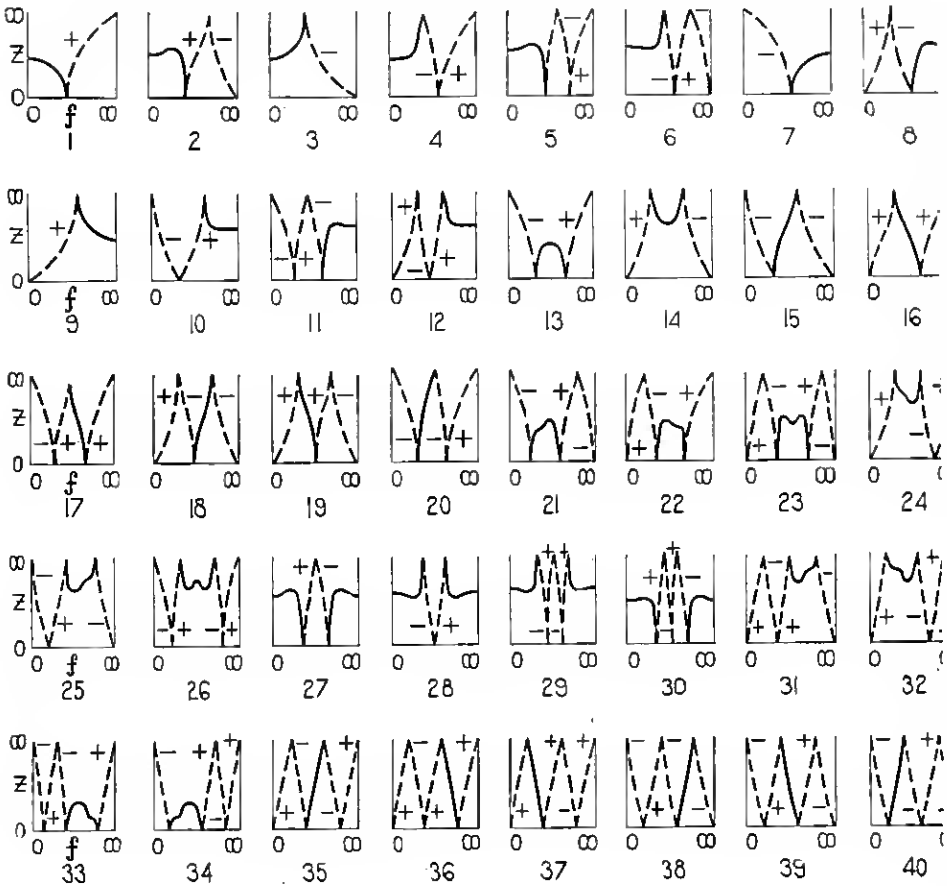

Fig. 8—Mid-Series and Mid-Shunt Image Impedance Characteristics, Shown in Symbolic Form

listed in Table II, and are called *low pass*, *high pass*, and *band pass* filters (having only one transmission band) and *band elimination*

[9] The general method of deriving the attenuation and phase characteristics of a section from the reactance-frequency characteristics of its series and shunt arms is discussed by Zobel in Bibliography 13.

Tabulation of the Propagation and Impedance Characteristics of Series-Shunt Wave Filter Sections Which can be Formed by the Reactance Meshes Shown in Fig. 5

SERIES ARM

SHUNT ARM	1	2	3	4	5	6	7	8
1	No Pass Band	3–7–9	6–13–16	4–8–9	9–22–16	Band-and-High Pass	Double Band Pass	Band-and-High Pass
2	1–1–3	No Pass Band	7–13–15	2–2–3	Low-and-Band Pass	10–21–15	Double Band Pass	Low-and-Band Pass
3	2–1–4	4–7–11	9–13–17 10–13–20	14–27–28	2–5–4	4–11–10	9–33–17 10–34–20	14–30–28
4	7–16–14	6–15–14	5–13–14	9–18–14 10–19–14	12–22–14	11–21–14	Triple Band Pass	8–23–14
5	10–16–24	Band-and-High Pass	11–13–24	4–8–12	9–22–36 9–35–24 10–22–35 10–37–24	Double Band-and-High Pass	More Than Six Elements	More Than Six Elements
6	Low-and-Band Pass	9–15–25	12–13–25	2–2–6	Low-and-Double Band Pass	9–21–39 9–38–25 10–21–40 10–39–25	More Than Six Elements	More Than Six Elements
7	Low-and-Band Pass	Band-and-High Pass	8–13–26	14–27–29	More Than Six Elements	More Than Six Elements	More Than Six Elements	More Than Six Elements
8	Double Band Pass	Double Band Pass	Triple Band Pass	9–18–31 10–19–32	More Than Six Elements	More Than Six Elements	More Than Six Elements	More Than Six Elements

filters (having two pass bands and only one attenuation band). Their attenuation constant and phase constant characteristics, with respect to frequency, are shown symbolically in Fig. 7. The mid-series and mid-shunt image impedance characteristics with respect to frequency are shown in Fig. 8. In Table II, the figure at the head of each column indicates the reactance mesh in Fig. 5 which is used for Z_1 (series impedance) and the figure at the left of each row indicates the mesh in Fig. 5 which is used for Z_2 (shunt impedance). The figures in the squares of the table denote, reading from left to right, the propagation characteristics (attenuation and phase), the mid-series image impedance, and the mid-shunt image impedance, respectively, as shown in Figs. 7 and 8.

For example, the filter corresponding to the third column and to the fourth row (3—4) has a series arm composed of an inductance in series with a capacity as indicated by mesh 3 of Fig. 5, and has a shunt arm composed of an inductance in parallel with a capacity, as designated by mesh 4 of Fig. 5. The attenuation constant and phase constant characteristics of this filter are shown symbolically by diagram 5 of Fig. 7, while the mid-series and mid-shunt image impedances are indicated, respectively, by diagrams 13 and 14 of Fig. 8. The symbolic nature of the diagrams lies in the fact that the abscissae of each diagram cover the frequency range from zero to infinity, and the ordinates of Figs. 7 and 8 cover the attenuation constant and the impedances from zero to infinity. For example, the structure cited has an attenuation constant characteristic (diagram 5 of Fig. 7) composed of a transmission band lying between two attenuation bands, the attenuation constant being infinite in one of them at zero frequency, and in the other, at infinite frequency. The phase constant of this structure is $-\pi$ radians in the lower of the two attenuation bands, increases from $-\pi$ to $+\pi$ radians in the transmission band (passing through zero), and is $+\pi$ radians throughout the upper of the two attenuation bands. The mid-series image impedance (diagram 13 of Fig. 8) is a negative reactance in the lower of the two transmission bands, decreasing from infinity, at zero frequency, to zero at the lower cut-off frequency, is a pure resistance throughout the transmission band, and is a positive reactance, increasing from zero to infinity, in the upper of the two attenuation bands. The mid-shunt image impedance characteristic (diagram 14 of Fig. 8) is reciprocal in nature, for this structure, to the mid-series image impedance characteristic. This type of filter also possesses, in the general case, a double band pass attenuation characteristic and corresponding phase and impedance characteristics. A discussion of such

characteristics is outside the scope of this paper even though many of the structures listed in Table II will show, if completely analyzed, multi-band characteristics. Where no specific characteristics are listed in Table II, no low pass, high pass, single band pass, or single band elimination characteristics are obtainable with a filter section limited to six different reactance elements.

In Table II, a large number of the structures have identically the same types of attenuation constant and phase constant characteristics. For example, six of the seven low pass filter sections have attenuation constant and phase constant characteristic No. 2 of Fig. 7. Likewise, six of the high pass structures have attenuation constant and phase constant characteristic No. 4. Also, in Table II, band pass groups are to be found having respectively, the following propagation characteristics common to each group: 6, 7, 8, 9, 10, 11 and 12. Finally, ten of the eleven band elimination structures listed have propagation constant characteristic No. 14.

Although six of the seven low pass wave filters have the same attenuation constant and phase constant characteristics, the various image impedance characteristics differentiate the structures among themselves. Similar differentiations exist in the high pass, band pass, and band elimination groups of structures. In each of the four types of filter sections however, all of those structures having the same series reactance meshes (that is, having the same series configuration of reactance elements) may be designed to have the same mid-series image impedance characteristic and, similarly, all of those structures within each type having the same shunt reactance meshes, or configuration of elements, may be designed to have the same mid-shunt image impedance characteristic.

In view of the fact that some of the structures listed in Table II have the same attenuation and phase constants but have different impedance characteristics, the question arises as to the relative virtues of the latter. Furthermore, since certain of the structures have the same mid-series or mid-shunt image impedances but have different propagation characteristics, it is possible to join together such structures and obtain a composite structure which has no internal reflection losses, that is, one whose total transfer constant is the sum of the various transfer constants of the individual sections. In order to minimize reflection and interaction losses in the transmission range, it is generally desirable to use, at the terminals of the filter, sections whose image impedances closely simulate those of the terminal impedances to which the filter is connected. The choice presented by

filter structures having different impedance characteristics but the same propagation characteristic is, therefore, of advantage. In the attenuation range this is also true where impedance conditions are imposed at the terminals of the filter.

One class of structures which possess desirable image impedances and whose characteristics are readily determined from simpler structures is the so-called derived m-type.[5] The simplest forms of derived

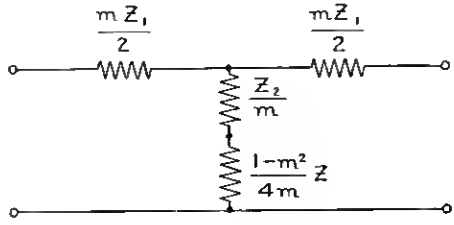

Fig. 9—Mid-Series Equivalent m-Type of Section

structures are shown in Figs. 9 and 10. The structure of Fig. 9 has the same mid-series image impedance as that shown in Fig. 2 and the value of this impedance is given by equation (6). The structure of Fig. 10 has the same mid-shunt image impedance as the π structure shown in Fig. 4 and the value of this impedance is given by

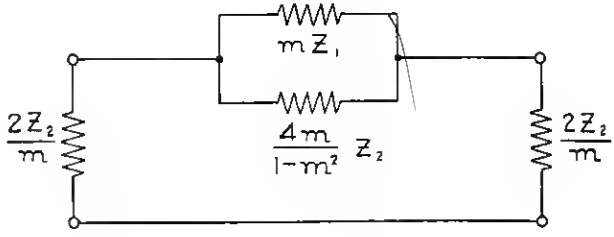

Fig. 10—Mid-Shunt Equivalent m-Type of Section

equation (7). On account of this identity of the respective mid-series and the mid-shunt image impedances in the two cases, the structures shown in Figs. 9 and 10 are called, respectively, the *mid-series equivalent derived* m-type and the *mid-shunt equivalent derived* m-type. The T and π structures of Figs. 2 and 4 are called, respectively, the *prototypes* of the derived m-structures of Figs. 9 and 10. In a series-shunt filter composed of sections of the m-type of Fig. 9 or Fig. 10,

the ratio $(Z_1/4Z_2)_m$ of the series impedance to four times the shunt impedance is

$$\left(\frac{Z_1}{4Z_2}\right)_m = \frac{m^2\left(\frac{Z_1}{4Z_2}\right)}{1+(1-m^2)\left(\frac{Z_1}{4Z_2}\right)}. \tag{21}$$

From this expression, when $Z_1/4Z_2$ of the prototype is 0 or -1, the corresponding value of $(Z_1/4Z_2)_m$ for the derived m-type is also 0 or -1. Hence, the derived type has the same cut-off frequencies and

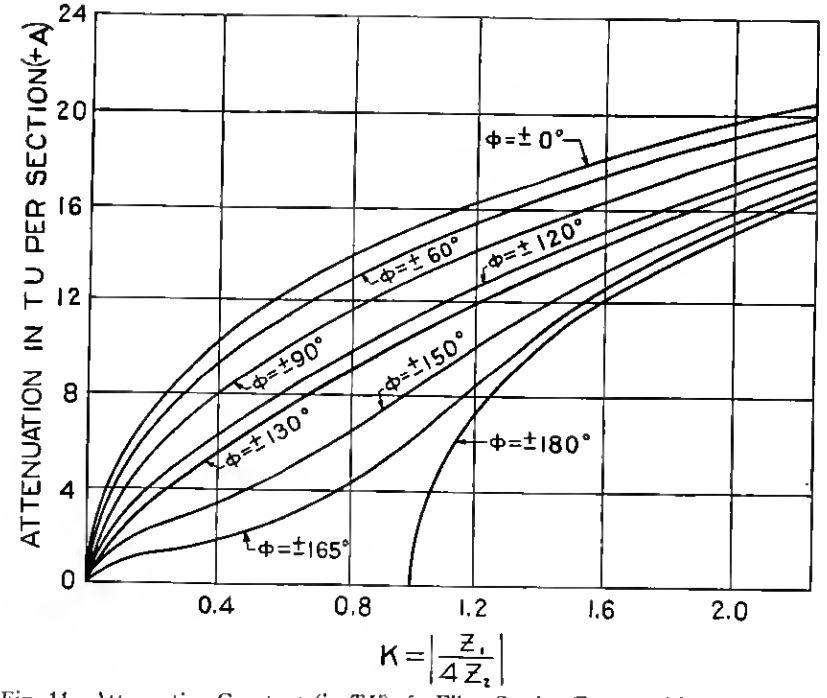

Fig. 11—Attenuation Constant (in *TU*) of a Filter Section Expressed in Terms of the Ratio of Its Series Impedance to Four Times Its Shunt Impedance (i.e., $Z_1/4Z_2 = K/\underline{\Phi}$)

therefore the same transmission and attenuation regions as its prototype.

Impedance and Propagation Characteristics of Dissipative Filters. It has been pointed out, in the case of non-dissipative structures, that the ratio $Z_1/4Z_2$ is either a positive or a negative numeric. If there is dissipation in the filter structure, that is, if the resistance associated with the reactance elements cannot be neglected, then the ratio

$Z_1/4Z_2$ will not, in general, be a numeric but a vector. However, the general formula (8), still holds true with dissipation. For determining the attenuation constant and phase constant of a dissipative structure it is convenient to use two formulae which may be derived from (8). These formulae are

$$A = \cosh^{-1}\left(K + \sqrt{(K-1)^2 + 4K\cos^2\frac{\phi}{2}}\right), \tag{22}$$

$$B = \cos^{-1}\left(-K + \sqrt{K^2 + 2K\cos\phi + 1}\right), \tag{23}$$

where

$$\frac{Z_1}{4Z_2} \equiv \left|\frac{Z_1}{4Z_2}\right| \angle \pm\phi \equiv K\angle \pm\phi.$$

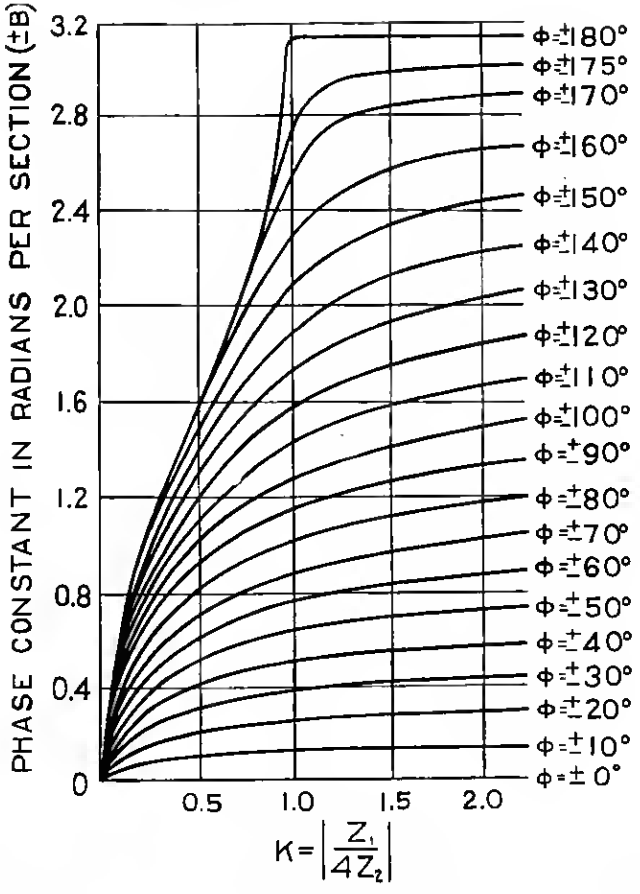

Fig. 12—Phase Constant of a Filter Section Expressed in Terms of the Ratio of Its Series Impedance to Four Times Its Shunt Impedance (i.e., $Z_1/4Z_2 \equiv K\angle\Phi$)

Formulae (22) and (23) are expressed in napiers and circular radians, respectively. They are represented in *TU* and in radians by families of curves such as are shown in Figs. 11 and 12.

A convenient ratio which expresses the dissipation in any reactance element is the absolute ratio, d, of its effective resistance to its reactance. In the case of a coil, $d=R/L\omega$ while in the case of a condenser $d=RC\omega$. The reciprocal ratio $Q\equiv\frac{1}{d}=\frac{L\omega}{R}=\frac{1}{RC\omega}$ has also been widely used as a measure of dissipation in reactance elements. The ratio d or Q will not, in general, be constant over a wide frequency

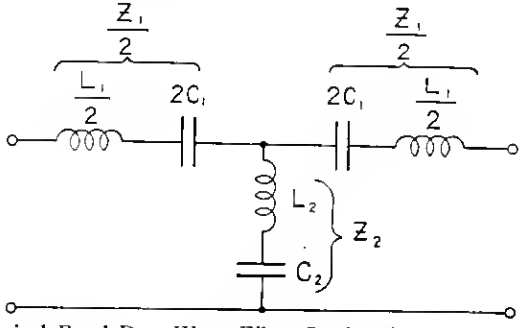

Fig. 13—Typical Band Pass Wave Filter Section (Mid-Series Termination)

range. If the value is known at an important frequency in the transmission range, it may ordinarily be regarded to hold for the rest of the transmission range. The effect of dissipation on the attenuation constant is most important in the transmission band, where the attenuation constant would be zero if there were no dissipation. Its effect is most pronounced in the neighborhood of the cut-off frequencies where the transmission bands merge into attenuation bands.

In the attenuation bands, the general effect of dissipation is negligible. It largely controls, however, the value of the attenuation constant at those frequencies at which infinite attenuation would occur if there were no dissipation. The effect of dissipation upon the phase constant is most pronounced in the neighborhood of the cut-off frequencies where resistance rounds off the abrupt changes in phase which would otherwise occur (see Fig. 12).

Characteristics of a Typical Filter. In order to illustrate specifically the principles employed in filter design, consider as an example the band pass structure 3−3 of Table II. This structure is illustrated in Fig. 13. It will be assumed that the dissipation in the coils cannot be neglected, but that the dissipation in the condensers is of negligible

magnitude. If R_1 and R_2 are the effective resistances of the inductance elements L_1 and L_2, respectively, the series impedance, Z_1, of a series-shunt recurrent structure composed of sections of the type shown in Fig. 13 is

$$Z_1 = R_1 + j\left(\omega L_1 - \frac{1}{\omega C_1}\right). \tag{24}$$

The impedance of the shunt arm is

$$Z_2 = R_2 + j\left(\omega L_2 - \frac{1}{\omega C_2}\right). \tag{25}$$

In substituting for R_1 its value $L_1\omega d$ and for R_2 its value $L_2\omega d$, the ratio $Z_1/4Z_2$ becomes

$$\frac{Z_1}{4Z_2} = \frac{L_1}{4L_2}\,\frac{1 - jd - \dfrac{1}{\omega^2 L_1 C_1}}{1 - jd - \dfrac{1}{\omega^2 L_2 C_2}}. \tag{26}$$

Assuming d to be zero, the ratio $Z_1/4Z_2$ is

$$\frac{Z_1}{4Z_2} = \frac{C_2(\omega^2 L_1 C_1 - 1)}{4C_1(\omega^2 L_2 C_2 - 1)}. \tag{27}$$

Referring to Table II, the structure shown in Fig. 13 has two distinct attenuation and phase characteristics. These are, respectively, characteristics Nos. 9 and 10 of Fig. 7. These two sets of characteristics arise from the fact that the shunt arm may be resonant at a frequency less than, or greater than, the resonant frequency of the series arm. The two attenuation characteristics are inverse with respect to frequency. We shall, therefore, discuss only one of the two cases, namely, that in which the shunt arm resonates at a frequency greater than the resonant frequency of the series arm (that is, L_1C_1 is greater than L_2C_2). The frequency at which the shunt arm is resonant will be designated as f_∞, due to the fact that in a non-dissipative filter the attenuation constant is infinite at this point. In other words,

$$f_\infty = \frac{1}{2\pi\sqrt{L_2C_2}}. \tag{28}$$

It is evident that the frequency at which Z_1 is resonant is a cut-off frequency since Z_1, and therefore $Z_1/4Z_2$, is zero at this point. An inspection of graphical curves[10] drawn for Z_1 and $4Z_2$, under the above

[10] For an illustration of the construction of such curves see Bibliography 12, Fig. 7, also Bibliography 13, Fig. 2.

conditions, will show that this is the lower of the two cut-off frequencies (f_1), that is

$$f_1=\frac{1}{2\pi\sqrt{L_1C_1}}. \tag{29}$$

By equating $Z_1/4Z_2$ to -1 in equation (27) the upper cut-off frequency (f_2) is found to be

$$f_2=\frac{1}{2\pi}\sqrt{\frac{C_2+4C_1}{C_1C_2(L_1+4L_2)}}. \tag{30}$$

For these explicit relations for f_1, f_2 and f_∞, equation (26) may be rewritten

$$\frac{Z_1}{4Z_2}=\left(\frac{f_1}{f_\infty}\right)^2\frac{\left[\left(\frac{f_\infty}{f_2}\right)^2-1\right]\left[(1-jd)\left(\frac{f}{f_1}\right)^2-1\right]}{\left[1-\left(\frac{f_1}{f_2}\right)^2\right]\left[(1-jd)\left(\frac{f}{f_\infty}\right)^2-1\right]}. \tag{31}$$

When d is zero this equation becomes, for the non-dissipative case

$$\frac{Z_1}{4Z_2}=\frac{\left[1-\left(\frac{f_\infty}{f_2}\right)^2\right]\left[1-\left(\frac{f_1}{f}\right)^2\right]}{\left[1-\left(\frac{f_1}{f_2}\right)^2\right]\left[\left(\frac{f_\infty}{f}\right)^2-1\right]}. \tag{32}$$

From the preceding formulae and from the curves shown in Figs. 11 and 12, it is possible to read directly the attenuation constant and the phase constant for the structure shown in Fig. 13, at any frequency, provided the values of f_1, f_2 and f_∞ are known. The formulae for the dissipative case are of use mainly throughout the transmission bands and near the frequency f_∞. Elsewhere, the formulae for $Z_1/4Z_2$ for the non-dissipative structure may be employed without undue error. The preceding formulae have been derived in a direct manner, but may be obtained more simply by considering the structure of Fig. 13 to be a derived form of the structure 3—2 in Table II.

In order to minimize reflection loss effects, it is, as a rule, desirable to terminate a filter in an impedance equal to the image impedance of the filter at the mid-frequency,[11] (f_m) or at some other important frequency. From equation (6) and the values of Z_1 and Z_2, the mid-series image impedance (Z_o), at the mid-frequency in the non-dissipative case is

$$Z_o=\frac{1}{2}\left[\sqrt{\frac{L_1}{C_1}+4\frac{L_1}{C_2}}-\sqrt{\frac{L_1}{C_1}+4\frac{L_2}{C_1}}\right]. \tag{33}$$

[11] Defined as the geometric mean of the two cut-off frequencies f_1 and f_2; or $f_m \equiv \sqrt{f_1 f_2}$.

From formulae (6), (29), (30), and (33) the mid-series image impedance at any frequency is

$$Z_I = Z_o \sqrt{1 - \frac{\left(\frac{f}{f_m} - \frac{f_m}{f}\right)^2}{\left(\frac{f_2}{f_m} - \frac{f_1}{f_m}\right)^2}}. \tag{34}$$

An inspection of formula (34) indicates that the mid-series image impedance is symmetrical with respect to the mid-frequency, f_m.

In a similar way, the mid-shunt image impedance (Z_o') at the mid-frequency is

$$Z_o' = \sqrt{\frac{4L_1}{C_2\left(\frac{C_2}{C_1}+4\right)}} - \sqrt{\frac{4L_2}{C_1\left(\frac{L_1}{L_2}+4\right)}} \tag{35}$$

and the mid-shunt impedance, (Z_I'), at any frequency is

$$Z_I' = Z_o' \frac{1-\left(\frac{f}{f_\infty}\right)^2}{1-\left(\frac{f_m}{f_\infty}\right)^2} \sqrt{\frac{\frac{f_2}{f_1} - \left(\frac{f_m}{f}\right)^2}{\frac{f_2}{f_1} - \left(\frac{f}{f_m}\right)^2}} \tag{36}$$

It will be noted, that *if the values of the inductances and resistances of a filter are multiplied by any factor and if all the values of the capacities are divided by the same factor, the transmission loss-frequency characteristic is not changed*[12] (*neither are the cut-off frequencies, nor the frequencies of infinite attenuation*) *but the image impedances are multiplied by this factor.*

From the preceding formulae, explicit expressions may be derived for the values of L_1, C_1, L_2, and C_2. These expressions, which are given by Zobel,[5] in a slightly different form, are as follows:

$$L_1 = \frac{Z_o m}{\pi(f_2 - f_1)}, \tag{37}$$

$$C_1 = \frac{f_2 - f_1}{4\pi f_1^2 Z_o m}, \tag{38}$$

$$L_2 = \frac{Z_o}{\pi(f_2 - f_1)} \frac{1-m^2}{4m}, \tag{39}$$

$$C_2 = \frac{(f_2 - f_1)m}{\pi Z_o (f_2^2 - f_1^2 m^2)}, \tag{40}$$

[12] Since the value of the transfer factor, $\epsilon - \theta$, is dependent simply upon the ratio $Z_1/4Z_2$, it is evident from equation (10) that *the transmission loss caused by the insertion of any network in a circuit is dependent simply upon impedance ratios.* Consequently, the above theorem is quite general and applies not only to filters but to any passive network.

where

$$m = \sqrt{1 - \frac{\left(\frac{f_2}{f_1}\right)^2 - 1}{\left(\frac{f_\infty}{f_1}\right)^2 - 1}}. \tag{41}$$

As a numerical example of the determination of the constants of a filter section of the type under consideration, assume that the lower cut-off frequency, f_1, is 20,000 cycles, and that the upper cut-off frequency, f_2, is 25,000 cycles and that the frequency of infinite attenuation, f_∞, is 30,000 cycles. Assume, furthermore, that the value of the mid-series image impedance, Z_o, at the mid-frequency is 600 ohms. Then from formula (41), $m = .742$; hence from (37), $L_1 = .0284$ henry; from (38), $C_1 = .00224 \times 10^{-6}$ farad; from (39) $L_2 = .00577$ henry and from (40) $C_2 = .00486 \times 10^{-6}$ farad. Assuming $d = .01$, the value of $Z_1/4Z_2$ as given by formula (31) at f_m (22,360 cycles) is found to be $.305\underline{/176°.4}$. Referring to formula (22), in which $K = .305$ and $\phi = 176°.4$, or to the curves of Fig. 11, this value of $Z_1/4Z_2$ corresponds approximately to .041 napiers or .36 *TU*. Similarly, from equation (23), or from the curves of Fig. 12, this value of $Z_1/4Z_2$ gives 1.15 radians, or 67°, for the phase constant. At zero frequency, the value of $Z_1/4Z_2$ is, from equation (31), $.542\underline{/0°}$, which corresponds to 1.36 napiers or to 11.8 *TU*. Likewise, at infinite frequency, the value of $Z_1/4Z_2$ is $1.23\underline{/0°}$, which corresponds to an attenuation loss of 1.97 napiers or to 16.6 *TU*. From the curves of Fig. 12, the phase constant is zero both at zero and at infinite frequency.

Composite Wave Filters. It has previously been pointed out that certain groups of the structures listed in Table II have the same mid-series or mid-shunt image impedance characteristics but that the various structures in such a group may have different attenuation and phase constant characteristics.

If a filter is composed of any number of symmetrical or dissymmetrical sections, so joined together that the image impedances at the junction points of the sections are identical, the attenuation and phase constant characteristics of the composite structure so formed, are equal to the sum of the respective characteristics of the individual sections. Furthermore, the image impedances of the composite filter will be determined by the image impedances of the accessible ends of the terminating sections. The desirability of forming such composite filters arises from the fact that a better disposition of attenuation and phase can be obtained by employing, in one composite structure, a number of different types of the characteristics shown in Fig. 7.

The dissymmetrical networks ordinarily employed in composite structures are usually L type networks each of which may be regarded as one-half the corresponding symmetrical T or π network. Generalized forms of such networks are shown in Figs. 14A, B, and C. By joining two of these half-sections, such as are shown in Figs. 14B

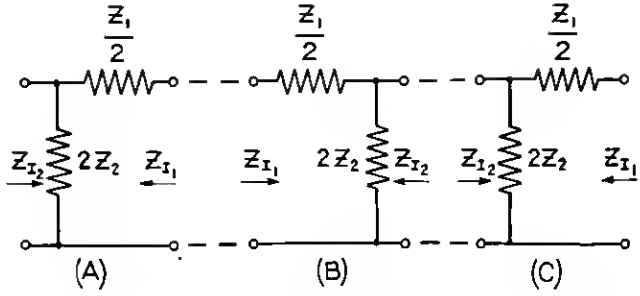

Fig. 14—Generalized Series-Shunt Structure Divided Into Successive Half-Sections (L-Type)

and C, we may form the full T section shown in Fig. 2. Similarly, by joining the two half-sections illustrated in Figs. 14A and B, the full π section of Fig. 4 results. The transfer constant, $\Theta_{\frac{1}{2}}$, of a half-section, such as is shown in Figs. 14A, B, or C, is one-half the transfer constant of the corresponding full section, that is,

$$\Theta_{\frac{1}{2}} = \frac{\Theta}{2} = \sinh^{-1}\sqrt{\frac{Z_1}{4Z_2}}. \tag{42}$$

Hence, the *attenuation constant and phase constant of a half-section* are, respectively, *one-half the attenuation constant and phase constant of a full section*. An important relationship between the half-section and the full section, which makes it convenient to use half-sections in composite wave filter structures, is that the image impedances, Z_{I_1} and Z_{I_2}, of any half-section are equal respectively to the mid-series and the mid-shunt image impedances of the corresponding full sections.

A typical example of the method of forming a composite low pass wave filter is given in Fig. 15, where three half-sections of different types and one full section are combined into a composite filter. The designations below the diagrams in Fig. 15A refer to the number of full sections and to the ratio f_∞/f_c. In a practical filter, the various shunt condensers and series coils are combined as illustrated in Fig. 15B.

The composite nature of the attenuation characteristic of the filter of Fig. 15B is illustrated in Fig. 16, on a non-dissipative basis. In

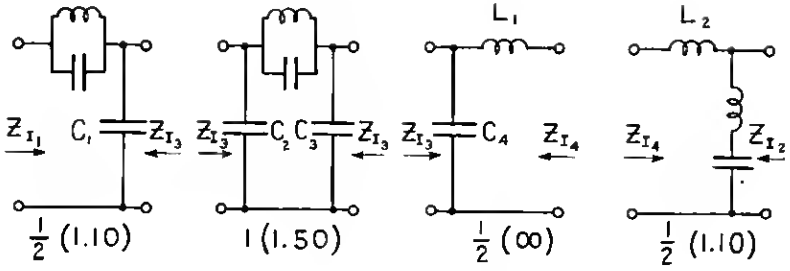

Fig. 15 A

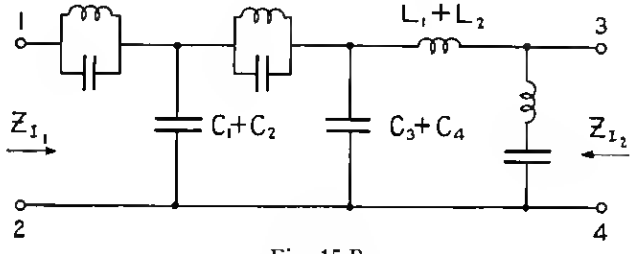

Fig. 15 B

Typical (Non-Dissipative) Composite Low Pass Wave Filter and Its Component Sections and Half-Sections

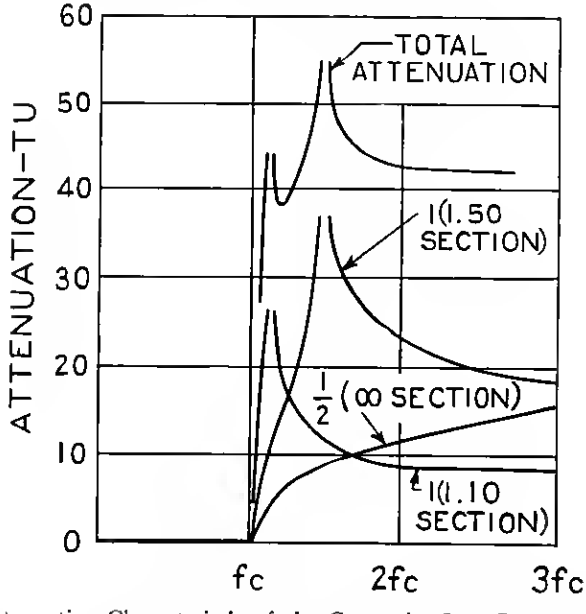

Fig. 16—Attenuation Characteristic of the Composite Low Pass Wave Filter of Fig. 15

Fig. 15B, the image impedance, Z_{I_1}, at the 1—2 terminals has characteristic No. 2 of Fig. 8, while the image impedance, Z_{I_2}, at the 3—4 terminals has characteristic No. 4 of Fig. 8.

Electrically Equivalent Networks. Reference has been made to the fact that *any passive network having one pair of input terminals and one pair of output terminals may be adequately represented, at any frequency, by an equivalent T or π network.* In general, this representation is a mathematical one and the arms of the T or π network cannot be represented, at all frequencies, by *physically realizable* impedances.

Furthermore, *any concealed network, containing no impressed electromotive forces, and having N accessible terminals is always capable of mathematical representation, at a single frequency, by a network having not more than* $N(N-1)/2$ *impedances, which impedances are determinable from the voltage and current conditions at the accessible terminals.* For networks having three or more terminals, this arbitrary mesh of impedances may possess a number of variant configurations. It is also true that the equivalence of the arbitrary mesh to the concealed network holds, at any single frequency, for any and all sets of external or terminal conditions, and that the magnitudes of the impedances of the arbitrary mesh are determinable, at will, on the assumption of the most convenient set of terminal conditions for each individual case. Familiar instances are the impedance equations derivable under various short-circuit and open-circuit conditions.

In specific cases, which are of particular interest, *one network may be shown to be capable of representation, as far as external circuit conditions are concerned, by another network which is physically realizable, and the latter may be substituted for the former, indiscriminately, in any circuit without consequent alteration, at any frequency, in the circuit conditions external to the interchanged networks.*

Equivalent meshes having two accessible terminals and employing respectively, three or four impedances in each mesh have been discussed by O. J. Zobel.[13] In filter design, two-terminal meshes are of importance only in those cases where the impedances are essentially reactances. Figs. 17A, B, C and D illustrate the physical configurations which reactance meshes employing not more than four elements may take. We are not generally interested in meshes having more than four elements for practical reasons which have previously been discussed. *Whenever any of the reactance meshes shown in Fig.* 17 *occur, we may, with proper design, substitute for it an equivalent mesh*

[13] See Appendix III of Bibliography 13.

of the associated type or types. Rigorous equivalence exists, *even with dissipation,* when the ratio of resistance to reactance, (d), is the same for all coils and the ratio of resistance to reactance (d') is the same for all condensers.

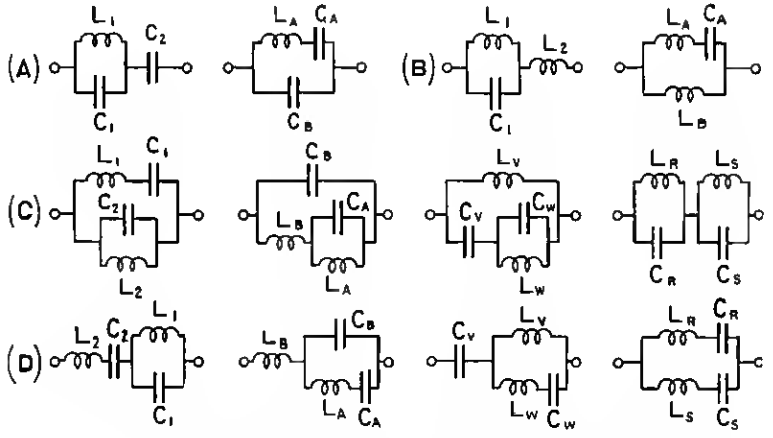

Fig. 17—Groups of Equivalent Two-Terminal Reactance Meshes

The relations which the equivalent meshes of Fig. 17 must observe are as follows:

17A

$$C_2 = C_A + C_B, \quad C_1 = \frac{C_B}{C_A}(C_A + C_B), \quad L_1 = \frac{L_A}{\left(1+\frac{C_B}{C_A}\right)^2}, \tag{43}$$

$$C_A = \frac{C_2^2}{C_1 + C_2}, \quad C_B = \frac{C_1\, C_2}{C_1 + C_2}, \quad L_A = L_1\left(1+\frac{C_1}{C_2}\right)^2, \tag{44}$$

17B

$$L_1 = \frac{L_B^2}{L_A + L_B}, \quad C_1 = C_A\left(1+\frac{L_A}{L_B}\right)^2, \quad L_2 = \frac{L_A\, L_B}{L_A + L_B}, \tag{45}$$

$$L_A = \frac{L_2}{L_1}(L_1 + L_2), \quad C_A = \frac{C_1}{\left(1+\frac{L_2}{L_1}\right)^2}, \quad L_B = L_1 + L_2, \tag{46}$$

17C

$$L_1 = \frac{L_B}{L_A}(L_A + L_B) = L_W\left(1+\frac{C_W}{C_V}\right)^2 = \frac{L_R L_S (L_R + L_S)(C_R + C_S)^2}{(L_R C_R - L_S C_S)^2} \tag{47}$$

$$L_2 = L_A + L_B = L_V = L_R + L_S, \tag{48}$$

17C

$$C_1=\frac{C_A}{\left(1+\frac{L_B}{L_A}\right)^2}=\frac{C_V^2}{C_V+C_W}=\frac{(L_RC_R-L_SC_S)^2}{(L_R+L_S)^2\,(C_R+C_S)}, \tag{49}$$

$$C_2=C_B=\frac{C_VC_W}{C_V+C_W}=\frac{C_RC_S}{C_R+C_S}, \tag{50}$$

$$L_A=\frac{L_2^2}{L_1+L_2},\ L_B=\frac{L_1L_2}{L_1+L_2},\ C_B=C_2, \tag{51}$$

$$C_A=C_1\left(1+\frac{L_1}{L_2}\right)^2,\ L_W=\frac{L_1}{\left(1+\frac{C_2}{C_1}\right)^2}, \tag{52}$$

$$L_V=L_2,\ C_V=C_1+C_2,\ C_W=\frac{C_2}{C_1}(C_1+C_2), \tag{53}$$

$$C_S=\frac{K+\sqrt{K^2-4L_2^2C_1C_2K}}{2L_2^2C_1}$$

$$\text{where } K=(L_1C_1+L_2C_1+L_2C_2)^2-4L_1C_1L_2C_2, \tag{54}$$

$$C_R=\frac{C_SC_2}{C_S-C_2},\ L_S=\frac{L_1C_1+L_2C_1+L_2C_2-L_2C_R}{C_S-C_R},\ L_R=L_2-L_S, \tag{55}$$

17D

$$C_1=\frac{C_B}{C_A}(C_A+C_B)=C_W\left(1+\frac{L_W}{L_V}\right)^2=\frac{C_RC_S(C_R+C_S)(L_R+L_S)^2}{(L_RC_R-L_SC_S)^2}, \tag{56}$$

$$C_2=C_A+C_B=C_V=C_R+C_S, \tag{57}$$

$$L_1=\frac{L_A}{\left(1+\frac{C_B}{C_A}\right)^2}=\frac{L_V^2}{L_V+L_W}=\frac{(L_RC_R-L_SC_S)^2}{(C_R+C_S)^2(L_R+L_S)}, \tag{58}$$

$$L_2=L_B=\frac{L_VL_W}{L_V+L_W}=\frac{L_RL_S}{L_R+L_S}, \tag{59}$$

$$C_A=\frac{C_2^2}{C_1+C_2},\ C_B=\frac{C_1C_2}{C_1+C_2},\ L_B=L_2, \tag{60}$$

$$L_A=L_1\left(1+\frac{C_1}{C_2}\right)^2,\ C_W=\frac{C_1}{\left(1+\frac{L_2}{L_1}\right)^2}, \tag{61}$$

$$C_V=C_2,\ L_V=L_1+L_2,\ L_W=\frac{L_2}{L_1}(L_1+L_2), \tag{62}$$

$$L_S=\frac{K+\sqrt{K^2-4L_1L_2C_2^2K}}{2L_1C_2^2}$$

$$\text{where } K=(L_1C_1+L_1C_2+L_2C_2)^2-4L_1C_1L_2C_2, \tag{63}$$

$$L_R=\frac{L_SL_2}{L_S-L_2},\ C_S=\frac{L_1C_1+L_1C_2+L_2C_2-L_RC_2}{L_S-L_R},\ C_R=C_2-C_S. \tag{64}$$

For example, the two meshes in Fig. 17A will be equivalent if

$C_1 = .009$ mf. $C_2 = .001$ mf. $L_1 = .001$ h.

$C_B = .0009$ mf. $C_A = .0001$ mf. $L_A = .100$ h.

and the two meshes in Fig. 17B will be equivalent if

$L_1 = .002$ h. $C_1 = .025$ mf. $L_2 = .008$ h.

$L_A = .040$ h. $C_A = .001$ mf. $L_B = .010$ h.

Also, the four meshes of Fig. 17C will be equivalent if

$L_R = .001$ h. $L_S = .002$ h. $C_R = .001$ mf. $C_S = .002$ mf.

$L_1 = .006$ h. $L_2 = .003$ h. $C_1 = .000333$ mf. $C_2 = .000667$ mf.

$L_A = .001$ h. $L_B = .002$ h. $C_A = .003$ mf. $C_B = .000667$ mf.

$L_V = .003$ h. $L_W = .000667$ h. $C_V = .001$ mf. $C_W = .002$ mf.

and the four meshes of Fig. 17D will be equivalent if

$L_R = .001$ h. $L_S = .001$ h. $C_R = .001$ mf. $C_S = .002$ mf.

$L_1 = .0000555$ h. $L_2 = .0005$ h. $C_1 = .024$ mf. $C_2 = .003$ mf.

$L_A = .0045$ h. $L_B = .0005$ h. $C_A = .000333$ mf. $C_B = .00267$ mf.

$L_V = .000555$ h. $L_W = .005$ h. $C_V = .003$ mf. $C_W = .00024$ mf.

It is then evident that the following reactance meshes of Fig. 5 may be designed to be equivalent: 5a and 5b; 6a and 6b; 7a, 7b, 7c, and 7d; and 8a, 8b, 8c, and 8d. Hence, the following filter sections

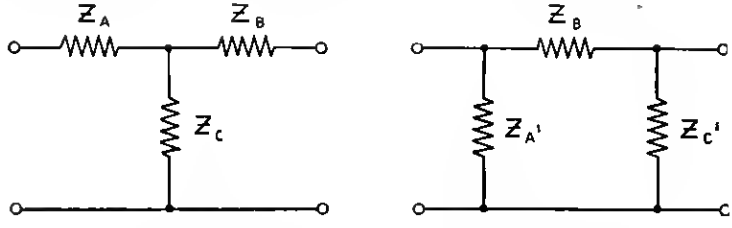

Fig. 18—Equivalent T and π Generalized Networks

referred to in Table II have, for the same impedance and propagation characteristics, a number of variant forms of physical configuration. 4–6, 6–2, 3–5, 6–4, 2–6, 5–3, 4–5, 1–5, 3–6, 5–4, 5–1, 4–8, 5–5, 6–6, 7–3, 6–3, 3–7, 4–7, 8–4 and 8–3.

Of the equivalent meshes having three accessible terminals the most common are the familiar T and π networks. The general relationships which must be observed for the equivalence of T or π net-

works are due to Kennelly [14] and for their generalized form, as illustrated in Fig. 18, are as follows:

$$Z_A = \frac{Z_A' Z_B'}{Z_A' + Z_B' + Z_C'}, \quad Z_B = \frac{Z_B' Z_C'}{Z_A' + Z_B' + Z_C'}, \quad Z_C = \frac{Z_A' Z_C'}{Z_A' + Z_B' + Z_C'}, \tag{65}$$

$$Z_A' = Z_A + Z_C + \frac{Z_A Z_C}{Z_B}, \; Z_B' = Z_A + Z_B + \frac{Z_A Z_B}{Z_C}, \; Z'_C = Z_B + Z_C + \frac{Z_B Z_C}{Z_A}. \tag{66}$$

We shall discuss here only two of the principal reactance meshes of the T and π form, namely, those employing solely inductances and

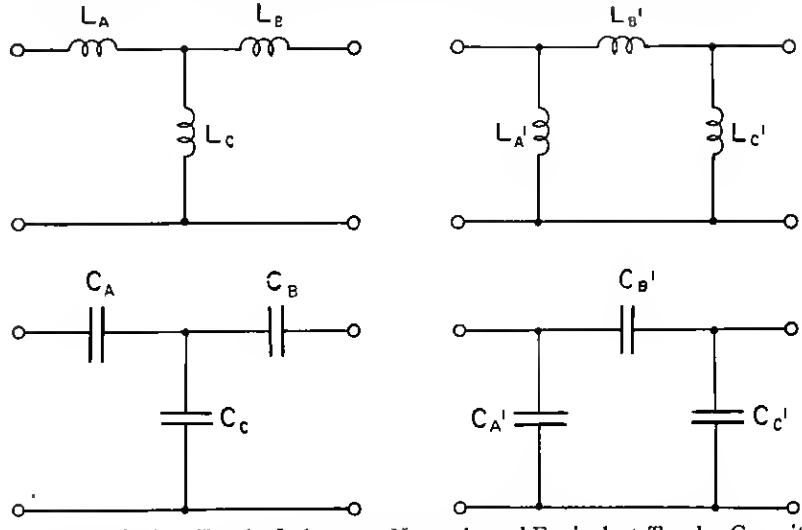

Fig. 19—Equivalent T and π Inductance Networks and Equivalent T and π Capacity Networks

solely capacities. It is to be understood that wherever an inductance or a capacity mesh of any of the following types occurs, its variant network may be substituted for it without change in the electrical characteristics of the circuit excluding those conditions within the mesh or its variant. Fig. 19 illustrates equivalent T and π networks of inductance and capacity.[15] The formulae relating the inductance and capacity meshes of Fig. 19 are as follows:

$$L_A = \frac{L_A' L_B'}{L_A' + L_B' + L_C'}, \quad L_B = \frac{L_B' L_C'}{L_A' + L_B' + L_C'}, \quad L_C = \frac{L_A' L_C'}{L_A' + L_B' + L_C'}, \tag{67}$$

[14] Kennelly, A. E., "The Equivalence of Triangles and Three-Pointed Stars in Conducting Networks," *Electrical World and Engineer*, New York, Vol. XXXIV, No. 12, pp. 413–414, Sept. 16, 1899. Also, "Application of Hyperbolic Functions to Electrical Engineering" (1911) (Appendix E).

[15] These meshes are rigorously equivalent, even when resistance is present if the ratio d is the same for all of the inductances and if the ratio d' is the same for all of the capacities.

$$L_A' = L_A + L_C + \frac{L_A L_C}{L_B}, \quad L_B' = L_A + L_B + \frac{L_A L_B}{L_C}, \quad L_C' = L_B + L_C + \frac{L_B L_C}{L_A}, \tag{68}$$

$$C_A' = \frac{C_A C_C}{C_A + C_B + C_C}, \quad C_B' = \frac{C_A C_B}{C_A + C_B + C_C}, \quad C_C' = \frac{C_B C_C}{C_A + C_B + C_C}, \tag{69}$$

$$C_A = C_A' + C_B' + \frac{C_A' C_B'}{C_C'}, \quad C_B = C_B' + C_C' + \frac{C_B' C_C'}{C_A'},$$

$$C_C = C_A' + C_C' + \frac{C_A' C_C'}{C_B'}. \tag{70}$$

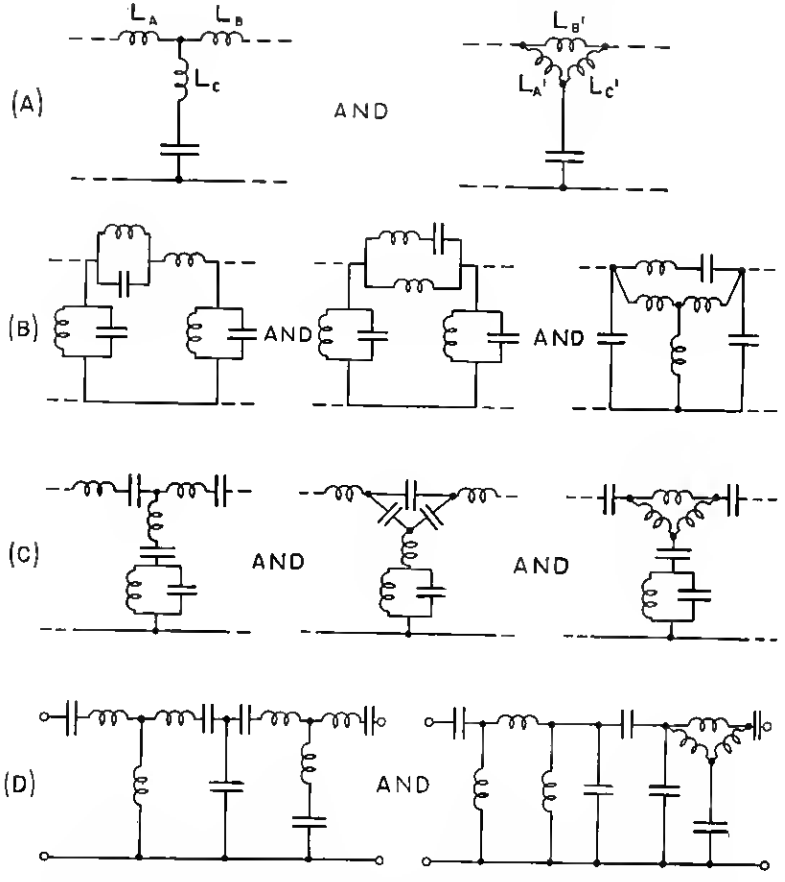

Fig. 20—Typical Examples of Equivalent Filters Involving the Interchange of Three-Terminal Networks of Inductances or of Capacities

A few examples of the variant filter structures which may arise, due to the existence of equivalent three terminal meshes of capacity

and inductance, are illustrated in Fig. 20, in which Figs. 20A, B, and C represent either individual sections or portions of composite filters and Fig. 20D represents a composite filter. When equivalent reactance meshes occur entirely within a filter or within a section of a filter, the filter or the section will have the same cut-off frequencies and frequencies of infinite attenuation and the same attenuation, phase, and image impedance characteristics, whichever equivalent

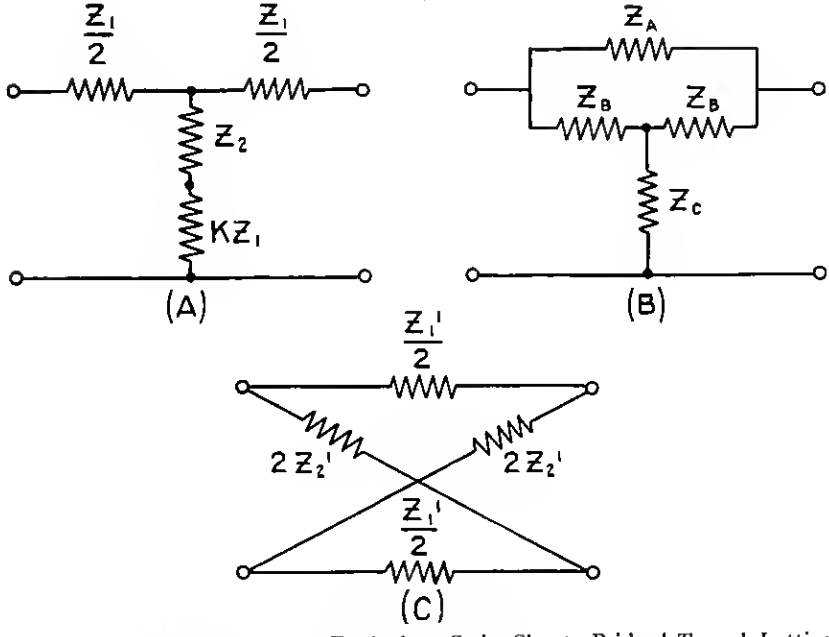

Fig. 21—Generalized Forms of Equivalent Series-Shunt, Bridged-*T*, and Lattice Type Filter Structures

form of mesh is substituted for an existing mesh. When equivalent meshes are interchanged in either recurrent or composite filters the substitution is generally made after the series-shunt structure is designed and after it has been found that the substitution will effect economies. The three terminal meshes referred to occur, in general, in unbalanced filter structures. For balanced filter circuits, corresponding meshes will be found for each of the equivalent networks by the process of dividing equally the series impedance between the two series lines of the filter.

While the discussion in this paper is based principally on the series-shunt structure there are two other important types of structures which will be mentioned. These are the so-called *lattice* [5] type struc-

ture and the *bridged-T* type structure. Typical series-shunt, bridged-T, and lattice type structures are illustrated in Fig. 21A, B and C, respectively. The three circuits shown are electrically equivalent, except for balance between the series arms, if the following relations hold:

$$Z_A = \left(1+\frac{1}{4K}\right)Z_1, \qquad Z_B = (\tfrac{1}{2}+2K)Z_1, \qquad Z_C = Z_2, \tag{71}$$

$$Z_1' = Z_1, \qquad Z_2' = (\tfrac{1}{4}+K)Z_1+Z_2. \tag{72}$$

In the previous discussion of equivalent networks no reference has been made to networks containing mutual inductance, many of which are of particular interest and importance. These will be now discussed in detail.

PART II

Wave Filters Using Mutual Inductance

Before considering the equivalent meshes which may be formed by the use of mutual inductance between pairs of coils, and the types of wave filters which may be obtained by the use of these equivalent meshes, it will be necessary to define certain general terms.

The *self impedance* between any two terminals of an electrical network is the vector ratio of an applied e.m.f. to the resultant current entering the network when all other accessible terminals are free from external connections.

The *mutual impedance* of any network, having one pair of input terminals and one pair of output terminals, is the *vector ratio* of the e.m.f. produced at the output terminals of the network, on open circuit, to the current flowing into the network at the input terminals. Since mutual impedance is a vector ratio, it may have either of two signs, depending on the assumed directions of the input current and the output voltage. The sign of the mutual impedance is, in general, identified by its effect in increasing or decreasing the vector impedance of the meshes in which it exists. It is usually convenient, in this case, to consider either a simple series or a simple parallel mesh of two self impedances between which the mutual impedance acts. For the purpose of determining the sign of the mutual impedance, we shall confine our discussion to a simple series combination. Consequently, the mutual impedance will be called either *series aiding* or *series opposing*.

When a mutual impedance, Z_M, acts between two self impedances Z_1 and Z_2, (Fig. 22) connected in series in such a way as to *increase vectorially* the impedance of the combination, it is called a *series aiding*

losses) the arms of its equivalent T network are composed simply of positive or negative inductances. Of the three inductances involved, at least two of them must be positive while the third may be either positive or negative.

From Fig. 25, it is evident that two windings or coils, together with their mutual impedance, may be represented by an equivalent network which affords a transfer of energy from one winding to the other. This equivalent network may, with limitations, contain positive or negative inductances.

While the two-winding transformer of Fig. 23 has been represented by an equivalent T network in Fig. 26, the equivalent network may alternatively be of π form (Fig. 27) instead of T form, through the

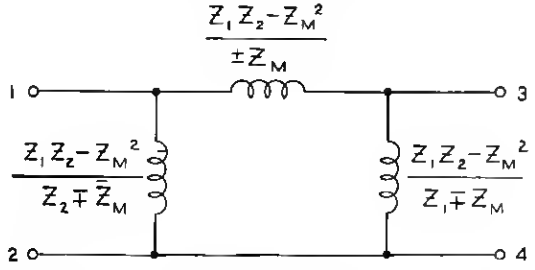

Fig. 27— π Network of Self Impedances Equivalent to the Structure of Fig. 23

general relationships for T or π networks previously stated. When no dissipation exists in the transformer, either equivalent network will have at least two positive inductances while the third inductance may be either positive or negative.

From the principles previously outlined in Part I, for the equivalence of certain electrical meshes and for their substitution for one another in any circuit, it is obvious that when two coils, with mutual impedance between them, exist in a circuit, in the manner shown in Fig. 23, either of the meshes shown in Fig. 26 or 27 may be substituted for them or vice versa. The representation of the mutual impedance, Z_M, by an equivalent network (Fig. 25) makes it possible to represent the transformer of Fig. 23 by a T or π network containing only self impedances. This affords a great simplification in the analysis of filter circuits containing pairs of coils having mutual impedance between them in that it permits such circuits to be reduced to an equivalent series-shunt (or lattice or bridged-T) type structure. Consequently, the methods of design which have been built up for the series-shunt and kindred type structures may be directly applied to the solution of circuits containing such pairs of coils.

Two-Terminal Equivalent Meshes. A list of equivalent two-terminal reactance meshes, due to Zobel, has been given in Fig. 17. All of the meshes in Figs. 17B, C and D contain two inductance elements. Mutual inductance may exist between any two inductive elements without changing fundamentally the nature of the reactance meshes. This means that when mutual inductance exists between two coils in

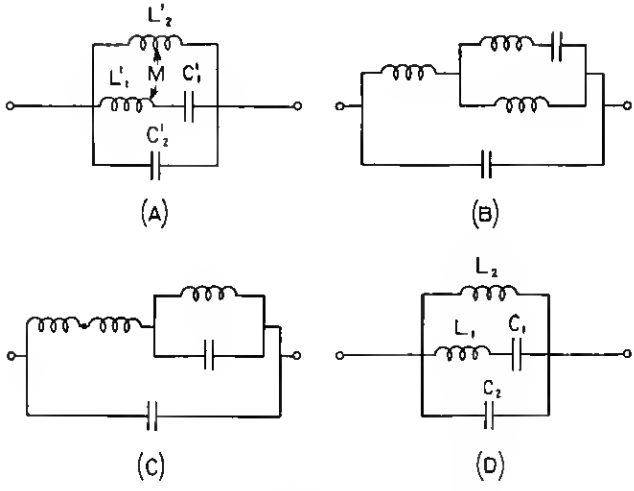

Fig. 28—Equivalent Two-Terminal Reactance Networks, Only One of Which Contains Mutual Inductance

any of these meshes, the mesh may be designed to be electrically equivalent to, and consequently can be substituted for, a corresponding mesh of the same type having no mutual inductance.

For example, consider the mesh shown in Fig. 28A which is potentially equivalent to the first reactance mesh of Fig. 17C and, consequently, to the other three reactance meshes of the same figure. The inductance elements L_1' and L_2', together with the mutual inductance M acting between them, may be represented by an equivalent T network, as previously stated. The reactance mesh formed by L_1', L_2', and M, together with its equivalent T and π forms, is shown in Fig. 29. By means of the relations given in Figs. 29A and B, it is possible to derive, from the structure of Fig. 28A, the equivalent structure shown in Fig. 28B. Likewise, from formulae (45) and (46) for the equivalence of the two structures of Fig. 17B, the mesh of Fig. 28C can be obtained from that of Fig. 28B. Furthermore, if the two inductances shown in series in Fig. 28C are merged, it is again possible, by means of the conversion formulae for the two meshes of

Fig. 17B, to determine the constants of the mesh shown in Fig. 28D from the known values of the constants of the structure of Fig. 28C.

The relations which must exist if the structure of Fig. 28D is to be equivalent to the structure shown in Fig. 28A, or vice versa, are given by the following relations

$$C_2 = C_2', \; L_1 = \frac{L_2'(L_1'L_2' - M^2)}{(L_2' \pm M)^2}, \tag{75}$$

$$L_2 = L_2', \; C_1 = C_1' \left(\frac{L_2' \pm M}{L_2'}\right)^2. \tag{76}$$

The upper and lower of the alternative signs, in the preceding equations, correspond respectively to series aiding and opposing connections. The equivalence of these four-element meshes makes it possible

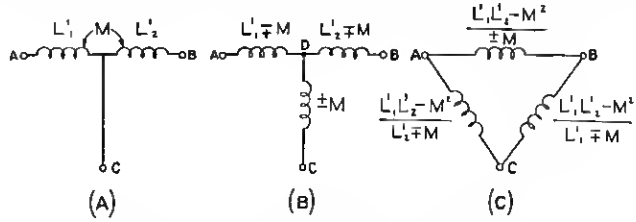

Fig. 29—Equivalent Three-Terminal Inductance Networks

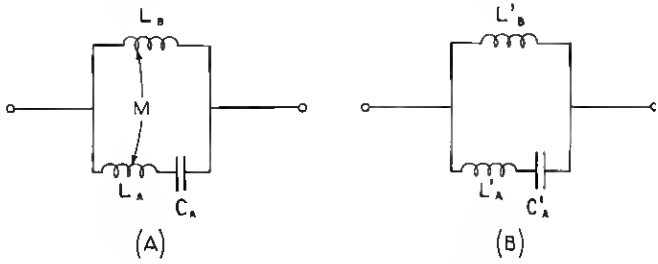

Fig. 30—Equivalent Two-Terminal Reactance Networks, Only One of Which Contains Mutual Inductance

to derive at once, the relations which must exist between certain equivalent three-element meshes involving mutual inductance. For example, if the capacity C_2' of Fig. 28A is zero, the mesh reduces to the three-element mesh of Fig. 30A and the formulae given above are then applicable for the equivalence of the structures of Figs. 30A and B.

In the same way that the meshes illustrated in Fig. 28 were shown to be potentially equivalent to each other, it is possible to prove that

the meshes of Fig. 31 are potentially equivalent. The equivalence of the mesh shown in Fig. 31B to that of Fig. 31A is satisfied by the relations given in Figs. 29A and B. The equivalence of the mesh of Fig. 31C to that of Fig. 31B is governed by the equations (56 to 64) for the equivalence of the first and last structures of Fig. 17D. Fin-

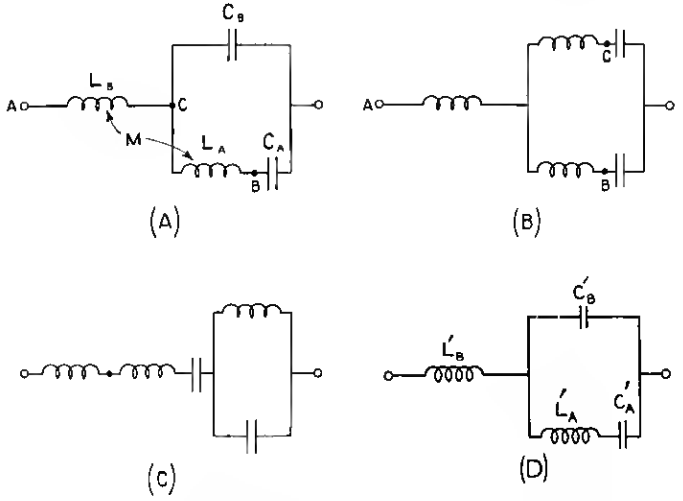

Fig. 31—Equivalent Two-Terminal Reactance Networks, Only One of Which Contains Mutual Inductance

ally, the equivalence of the mesh of Fig. 31D to that of Fig. 31C is controlled by the relations for the equivalence of the first two structures of Fig. 17D.

The formulae relating the constants of the structure shown in Fig. 31D to the corresponding constants of the structure shown in Fig. 31A are as follows:

$$L_A' = L_1\left(1+\frac{C_1}{C_2}\right)^2,\ L_B' = L_2,\ C_A' = \frac{C_2^2}{C_1+C_2},\ C_B = \frac{C_1C_2}{C_1+C_2}, \qquad (77)$$

in which—

$$C_1 = \frac{C_AC_B(C_A+C_B)L_A^2}{[C_A(L_A \pm M) \pm MC_B]^2},\ C_2 = C_A+C_B, \qquad (78)$$

and

$$L_1 = \frac{[C_A(L_A \pm M) \pm MC_B]^2}{(C_A+C_B)^2L_A},\ L_2 = \frac{L_AL_B-M^2}{L_A}. \qquad (79)$$

The upper and lower of the alternative signs, in the preceding equations correspond, respectively, to series aiding and opposing connections.

The equivalence of these four-terminal meshes makes it possible to derive the relations which must exist for corresponding equivalent three-element meshes, with and without mutual inductance. For example, if in Fig. 31A, the capacity C_A is of infinite value, the mesh reduces to that shown in Fig. 32A and the formulae given above are applicable for the equivalence of the meshes of Figs. 32A and B.

The remaining meshes of Figs. 17C and D have similar potential equivalence to meshes of the same fundamental type but having mutual inductance between the respective pairs of coils.

Three-Terminal Equivalent Meshes. Three terminal meshes containing mutual inductance will now be discussed. It has been shown

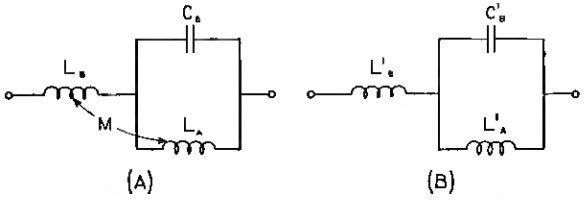

Fig. 32—Equivalent Two-Terminal Reactance Networks, Only One of Which Contains Mutual Inductance

that two coils, with mutual inductance between them (Fig. 29A), are equivalent to certain T and π structures containing only tangible inductances (Figs. 29B and C). Referring to Fig. 29B, it is seen that two coils, with series opposing mutual inductance between them (corresponding to the upper alternative signs in Fig. 29B), are equivalent to a T network having three positive inductance arms, provided the mutual inductance M is less than L_1' and L_2'. The values of these arms are respectively, $L_1'-M$, $L_2'-M$, and M. If M is larger than L_1', one arm of the equivalent T network is a negative inductance while the other two arms are positive inductances. Similarly, if M is larger than L_2', a different arm of the T network will be a negative inductance while the two remaining arms will be positive inductances. It is physically impossible for the value of M to be greater than both L_1' and L_2'. Hence, it is impossible for more than one arm of the T network, shown in Fig. 29B, to be a negative inductance.

When two coils have series aiding mutual inductance between them (the lower of the alternative signs in Fig. 29B) they are equivalent to a T network in which two of the arms consist of positive inductances viz., $L_1'+M$ and $L_2'+M$, while the third arm consists of a negative inductance of the value $-M$.

Whenever, in an equivalent T network, one of the arms is a positive (or negative) inductance, a corresponding arm of the π network will also be a positive (or negative) inductance. Consequently, as in the case of the equivalent T network, the equivalent π network shown in Fig. 29C may consist of three positive inductances or two positive inductances and one negative inductance, depending upon the sign and magnitude of M.

It is interesting to note that, in Fig. 29B, point D is in reality a concealed terminal, i.e., it cannot be regarded as physically accessible. There are, therefore, only three accessible terminals to the equivalent

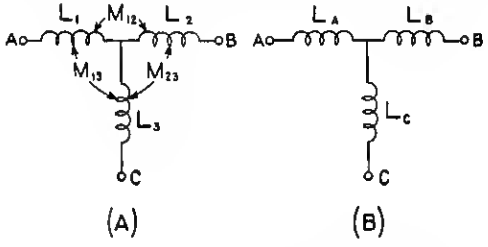

Fig. 33—Equivalent T Networks of Inductance

T network. In the π network shown in Fig. 29C there is no such concealed point. There are, however, as in the preceding case, three accessible terminals A, B and C.

When the mutual inductance, M, is equal to either one of the self inductances, L_1' (or L_2'), and the windings are connected in series opposing, the equivalent T and π networks of the transformer coalesce to the same L type network. For example, if $L_1' = M$ in Fig. 29A both the T and the π networks of Figs. 29B and C resolve into an L network whose vertical arm has the value M and whose horizontal arm is $L_2' - M$.

A problem of practical importance is the equivalence of T and π meshes, containing three coils with mutual inductance between all of the elements, to similar T and π meshes containing no mutual inductance. The T networks of Fig. 33 are potentially equivalent. The formulae governing their equivalence are

$$L_A = L_1 + M_{12} + M_{13} - M_{23}, \tag{80}$$

$$L_B = L_2 + M_{12} - M_{13} + M_{23}, \tag{81}$$

$$L_C = L_3 - M_{12} + M_{13} + M_{23}. \tag{82}$$

In the above formulae, the signs correspond to the case of a series aiding mutual inductance between all the pairs of coils. When the

mutual inductance between any two coils changes sign, the signs accompanying that mutual inductance in the above formulae are reversed.

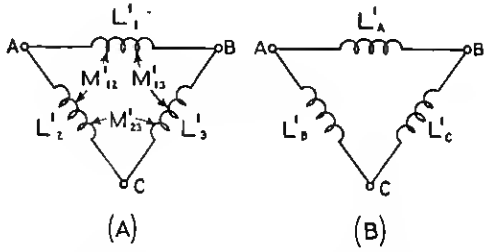

Fig. 34—Equivalent π Networks of Inductance

Similarly, the π networks of Fig. 34 are also potentially equivalent The formulae governing their equivalence are

$$L_A' = \frac{L_xL_y + L_xL_z + L_yL_z}{L_y}, \tag{83}$$

$$L_B' = \frac{L_xL_y + L_xL_z + L_yL_z}{L_z}, \tag{84}$$

$$L_C' = \frac{L_xL_y + L_xL_z + L_yL_z}{L_x}, \tag{85}$$

in which—

$$L_x = \frac{L_A''L_B''}{L_A'' + L_B'' + L_C''} \mp M_{12}', \tag{86}$$

$$L_y = \frac{L_B''L_C''}{L_A'' + L_B'' + L_C''} \mp M_{23}', \tag{87}$$

$$L_z = \frac{L_A''L_C''}{L_A'' + L_B'' + L_C''} \mp M_{13}', \tag{88}$$

where

$$L_A'' = L_1' \pm M_{12}' \pm M_{13}', \tag{89}$$

$$L_B'' = L_2' \pm M_{12}' \pm M_{23}', \tag{90}$$

$$L_C'' = L_3' \pm M_{13}' \pm M_{23}'. \tag{91}$$

As in the preceding case, the upper of the two signs occurs with the series aiding mutual inductance between all the pairs of coils. When the mutual inductance between any two coils changes sign, the signs accompanying that mutual inductance in the above formulae are reversed.

At least two of the three inductances (in Fig. 33B or in Fig. 34B) will always be positive in sign while the third inductance may be

either positive or negative. Consequently, three coils having mutual inductance between each of them and having only three accessible terminals offer no greater possibilities than do two coils having mutual inductance between them and having three terminals. In both cases the structure is equivalent to a T or π mesh composed of three self

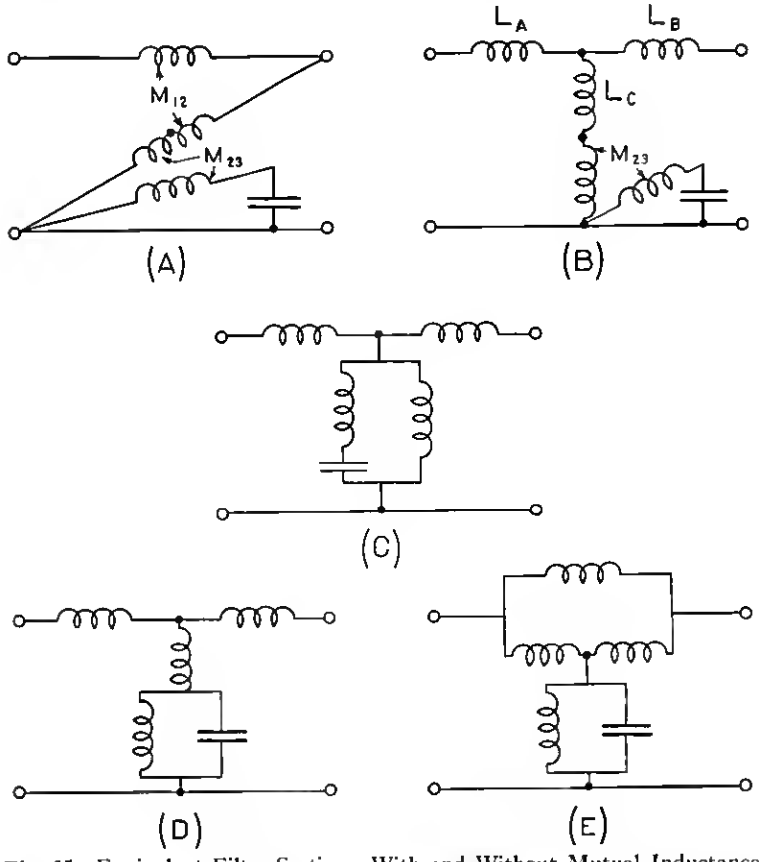

Fig. 35—Equivalent Filter Sections, With and Without Mutual Inductance

inductances, at least two of which must be positive. With specific relations between the various self and mutual inductances, it is possible for the three coils with mutual inductance between each of them to be equivalent (as in the case of two coils with mutual inductance) simply to an L network composed of two positive self inductances.

Since either two or three coils with mutual inductance between them are, in general, equivalent, at all frequencies, to a T or π net-

work composed of three self inductances, it is possible to substitute the one type of mesh for the other in any kind of a circuit without affecting the currents or voltages external to the meshes involved. This substitution is always physically possible provided none of the arms of the equivalent T or π networks is a negative inductance.

The structures shown in Fig. 35 are illustrative of the power of equivalent networks as tools for the solution of filter structures containing mutual inductance. The equivalence of the structure shown in Fig. 35B to that of Fig. 35A is evident from the equivalence of two coils (Fig. 29) with mutual inductance (M_{12}) between them to three inductances, L_A, L_B and L_C without mutual inductance. Likewise,

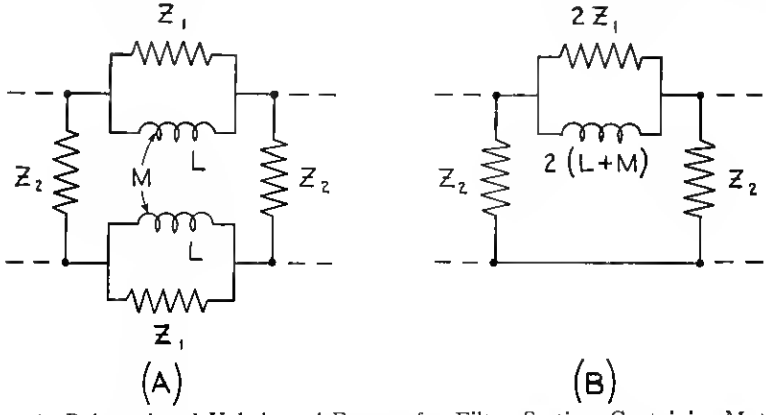

Fig. 36—Balanced and Unbalanced Forms of a Filter Section, Containing Mutual Inductance

the equivalence of the structure shown in Fig. 35C to that of Fig. 35B is obtainable by successive mesh substitutions. The equivalence of the structures shown in Fig. 35D and E to that of Fig. 35C are also obtainable from equivalences previously referred to. If the propagation and impedance characteristics of either of the structures of Fig. 35C or D are known, then the other structures shown in Fig. 35 will have the same characteristics. Furthermore, if the values of the constants of any one of these structures are known, the constants of any of the other structures are readily obtainable by means of transformation formulae.

In a large number of wave filters, the structures are unbalanced; that is, all of the series impedances are placed in one of the two line wires while the remaining wire is a short circuit. Ordinarily, the object in using such an unbalanced structure is to minimize the number of elements required in the series arms. It should be noted, however, (Fig. 36) that in case an inductance element enters into

both series arms, it can be replaced, in symmetrical structures, by two equal windings of a single coil having mutual inductance between them and of such value that the series aiding inductance of these two coils is equal to the total inductance required in the corresponding unbalanced structure. For example, the structures shown in Figs. 36A and B are electrically equivalent to each other, that is, they have the same image impedance and transfer constant.

Types of Sections Obtainable Whose Equivalent Series-Shunt Sections Contain No Negative Inductances. It has previously been stated that an infinite number of types of series-shunt filter sections may be had, if no limitations are placed on the complexity of their reactance arms. It has also been stated, however, that for filters employing only one transmission or one attenuation band, the maximum number of elements which can ordinarily be used economically per section is six. A similar limitation exists when mutual inductance is employed, in that sections can seldom be economically used whose prototype structures contain more than six reactance elements.

Inasmuch as by the equivalences which have been discussed, many varient forms of a section may exist, which forms are reducible to the same series-shunt prototype, an effort only to list and discuss the prototype sections will be made. The prototype to which any given section then reduces will readily be found by the application of the foregoing principles. A few examples will later serve to make this clear.

In considering the prototype sections which exist when mutual inductance is present in a filter section, we shall first list the reactance meshes of which mutual inductance may form a part. Referring to Fig. 5, an inspection of the equivalences so far discussed will show that the following meshes may be partly or wholly composed of mutual inductance:

1, 3, 4, 5 (*a* and *b*), 7 (*a* and *b*), and 8 (*a* and *b*).

Consequently, a large number of the sections listed in Table II and formed from the reactance meshes of Fig. 5 may represent *not only actual sections containing no mutual inductance, but also equivalent prototypes of sections containing mutual inductance.* Sections containing mutual inductance within only the series arm or the shunt arm, respectively, are not included in this discussion since such arms may be readily reduced to equivalent arms, without mutual inductances, by the substitution of equivalent two-terminal meshes. The prototypes which are under discussion are listed below:

Low pass	*High pass*
1−3, 5−3	4−1, 4−5

Band pass

3−1, 1−4, 3−3, 4−4, 1−5, 5−1, 3−7, 3−5, 8−4, 4−8, 5−4, 5−5, and 7−3.

Sections corresponding to the equivalent series-shunt prototypes listed will have the same impedance and propagation characteristics as the prototype, and may be used indiscriminately in place of the prototype. Consequently, when a section has been reduced to any of the above prototypes, its various characteristics may be found from Table II and Figs. 7 and 8.

As an example of structures which have mutual inductance and which are equivalent to structures listed above, consider the section

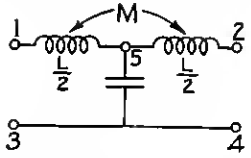

Fig. 37—Low Pass Filter Section Containing Two Coils, Having Mutual Inductance Acting Between Them, and a Condenser Shunted From Their Junction Point

shown in Fig. 37. This section contains two coils having mutual inductance, and a condenser shunted from their junction point. The three-terminal mesh formed by the two coils $L/2$ and $L/2$, together with their series opposing mutual inductance M, may be represented, as in Fig. 29B, by its equivalent T mesh. The resulting equivalent section is that shown in Fig. 38. The structure of Fig. 38, having a series reactance mesh corresponding to No. 1 of Fig. 5, and a shunt

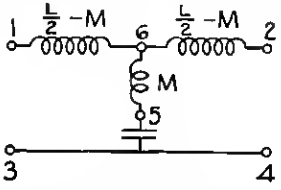

Fig. 38—Filter Section Containing No Mutual Inductance, Equivalent to the Section of Fig. 37

reactance mesh corresponding to No. 3 of Fig. 5 is that listed as 1−3 in Table II and in the above list. Consequently, it has propagation characteristic No. 2 of Fig. 7, and mid-series image impedance characteristic No. 1 of Fig. 8. The section of Fig. 37 may, consequently, be joined at either end to any structure having a mid-series image impedance characteristic such as that designated as character-

istic No. 1 of Fig. 8. The section of Fig. 37 is not capable of mid-shunt termination since point 6 of Fig. 38 is not physically accessible.

Similarly, the section shown in Fig. 39 is equivalent to the series-shunt structure of Fig. 40. If the transformer mesh in Fig. 39, formed by $2L_2$, M and $2L_2$ be replaced by its equivalent π mesh,—assuming series opposing windings—the structure of Fig. 40 results.

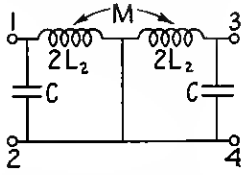

Fig. 39—Band Pass Filter Section Containing Mutual Inductance

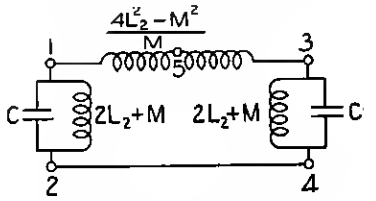

Fig. 40—Filter Section, Containing No Mutual Inductance, Equivalent to the Section of Fig. 39

This structure is listed as band pass section 1—4 in Table II and has propagation characteristic No. 7 of Fig. 7, and mid-shunt image impedance characteristic No. 14 of Fig. 8. Consequently, the section of Fig. 39 may be joined efficiently to any filter section of Table II having the mid-shunt image impedance characteristic No. 14 of Fig. 8 or to any section containing mutual inductance and having the same mid-shunt image impedance characteristic. The section of Fig. 39 is not capable of mid-series termination, since point 5 of inductive element 1—3 of Fig. 40 is not physically accessible.

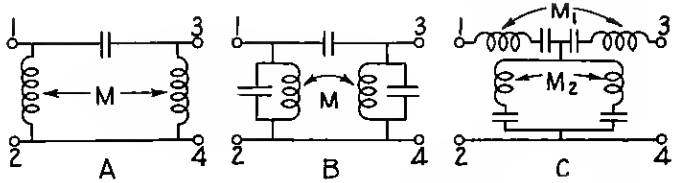

Fig. 41—Examples of Filter Sections Containing Mutual Inductance

Three further examples of the substitutions which have been discussed are represented in Figs. 41A, B, and C. By means of substitutions these structures are evidently equivalent to series-shunt sections 4—1 (mid-shunt terminated), 4—4, (mid-shunt terminated), and 3—7 (mid-series terminated), respectively, and they have the characteristics detailed in Table II. The above examples represent only a few of the many variant forms of structures which may be constructed by means of the various equivalences heretofore discussed.

The representation of the characteristics of the structures of Table III is similar to the scheme of Table II. The figures at the top and side (for example 1−3′) indicate respectively, the series and shunt reactance meshes of Figs. 5 and 42 which form the prototype sections.

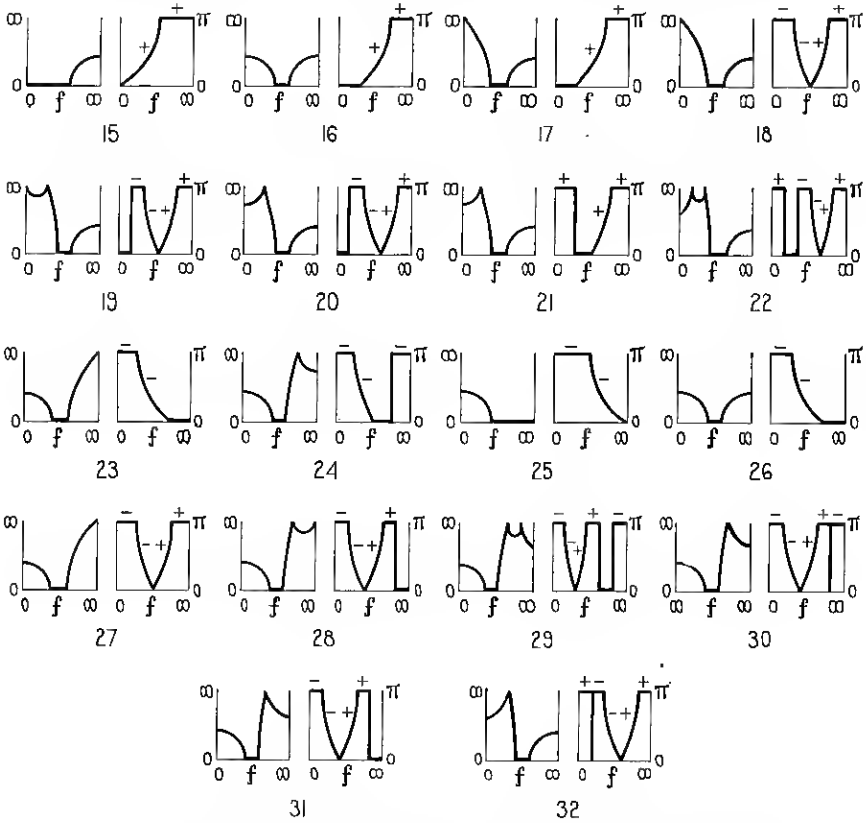

Fig. 44—Propagation Constant (Attenuation and Phase Constant) Characteristics of Filter Sections Containing Negative Inductances, Shown in Symbolic Form

The figures in the corresponding box (for example, 15−1−*) indicate that the structure has propagation characteristic No. 15 of Fig. 44, and mid-series image impedance No. 1 of Fig. 8. The symbol * indicates, when inserted in the second or third position, that the structure is not physically capable of mid-series or mid-shunt termination, respectively.

It will be noted that only one low pass prototype section (1−3′) is given in the table, exclusive of special cases of band filter structures.

Its attenuation characteristic (No. 15 of Fig. 44) is unique as a low pass characteristic in that *the attenuation constant is finite at all frequencies*. The phase characteristic simulates, in a general way, that of the two element low pass filter (see propagation characteristic No. 1 of Fig. 7) but the phase shift in the transmission band is, in general, different. Since the structure has mid-series image impedance characteristic No. 1 it may be joined efficiently (i.e., without reflection losses) to sections of the 1—2 and 1—3 types.

Similarly, high pass prototype section 4′—1 has a unique high pass attenuation characteristic in that the attenuation constant is finite at all frequencies. The phase characteristic is, in general, similar to that of the two element high pass filter 2—1 except for the values of the phase constant in the transmission band. The section may be joined efficiently at mid-shunt to sections of the 2—1 and 4—1 types—since it has the same mid-shunt image characteristic (No. 9).

The attenuation characteristics of the band pass prototypes listed in Table III will, in general, differ from the attenuation characteristics of structure listed in Table II. However, many of them differ only in minor respects and could have been represented identically in the symbolic fashion of Fig. 7. Inasmuch as such structures will not, however, have exactly the same attenuation characteristics for given cut-off frequencies and frequencies of infinite attenuation, different symbols or diagrams have been employed to represent them.

Certain characteristics are worthy of comment because they are not obtainable, even approximately, in structures not having negative inductance. For example, propagation characteristics Nos. 16 and 26 (Fig. 44) are band pass filter characteristics having finite attenuation at all frequencies. Characteristics No. 22 and No. 29 are unique in that there exist two frequencies of infinite attenuation, located on one side of the pass band. The attenuation constant is, in general, finite at zero and at infinite frequencies. Characteristics 19 and 28 are special cases of Nos. 22 and 29, respectively, and have two frequencies of infinite attenuation on one side of the pass band. In the case of 19, the attenuation is infinite at zero frequency and at a frequency between zero and the lower cut-off frequency. Characteristic 28 has infinite attenuation at infinite frequency and also at a frequency between the upper cut-off frequency and infinite frequency. Characteristics Nos. 18 and 27 have confluent band characteristics and have only one frequency of infinite attenuation, located either at zero frequency or at infinite frequency. Finally, characteristics Nos. 20 and 31 are confluent characteristics in each of which one fre-

quency of infinite attenuation occurs and the attenuation is finite at zero frequency and infinite frequency.

As a general rule the phase shift characteristics shown in Fig. 44 are similar to the corresponding characteristics shown in Fig. 7. The phase characteristics of the former, within the pass bands are, in general, however, of a distinctly different character than those of the latter even though the phase constant at the cut-off frequency and the mid-frequency may be the same. Phase characteristics 21 and 24 (Fig. 44) are of special interest, however, in that while they belong to the peak type sections, the phase is of the same sign throughout the entire frequency range. Also phase characteristics 22, 29, 30 and 32 have a unique property, for band pass structures, in that the phase undergoes a change in sign within one attenuation band.

In regard to the impedance characteristics, it is noted from Table III that *no novel impedance characteristics are obtained in structures having negative inductances as compared to the structures not having negative inductances.* This is a valuable property of the prototype structures listed in Table III as it permits composite filters to be readily formed utilizing both the sections of Tables II and III.[16]

Characteristics of a Typical Filter. In order to illustrate the derivation of design formulae for a specific prototype having negative inductances, consider as an example the band pass structure 3—3′ of Table III. We shall neglect the effect of dissipation on the characteristics of the structure, as the treatment of dissipation has been previously outlined. The prototype cited is illustrated in Fig. 45A. Two

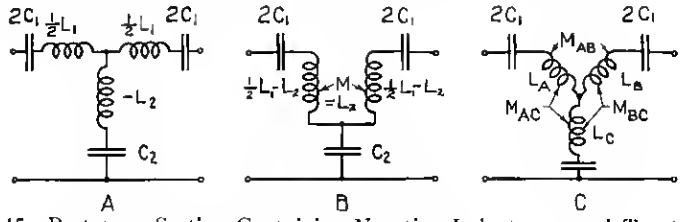

Fig. 45—Prototype Section Containing Negative Inductance, and Two of Its Physically Realizable Forms

methods of physically obtaining such a prototype are illustrated in Figs. 45B and C. In this structure the series impedance Z_1 is

$$Z_1 = j\left(\omega L_1 - \frac{1}{\omega C_1}\right). \tag{92}$$

[16] For a general method of proving the equality of the image impedances of sections containing negative inductance and of appropriate sections containing no negative inductance, refer to the Appendix.

The impedance of the shunt arm is

$$Z_2 = -j\left(\omega L_2 + \frac{1}{\omega C_2}\right). \tag{93}$$

The ratio, $Z_1/4Z_2$, which controls the attenuation and phase constants, per section, of the structure is

$$\frac{Z_1}{4Z_2} = \frac{j\left(\omega L_1 - \frac{1}{\omega C_1}\right)}{-j\left(\omega L_2 + \frac{1}{\omega C_2}\right)} = \frac{C_2}{4C_1}\,\frac{1-L_1C_1\omega^2}{1+L_2C_2\omega^2}. \tag{94}$$

From the impedance characteristics of reactance meshes 3 and 3′, as illustrated in Figs. 6 and 43, and the combined reactance characteristics of Fig. 46 for Z_1, $4Z_2$ and $-4Z_2$, it will be noted that the lower cut-off frequency, f_1, is that at which $Z_1 = 0$. Hence,

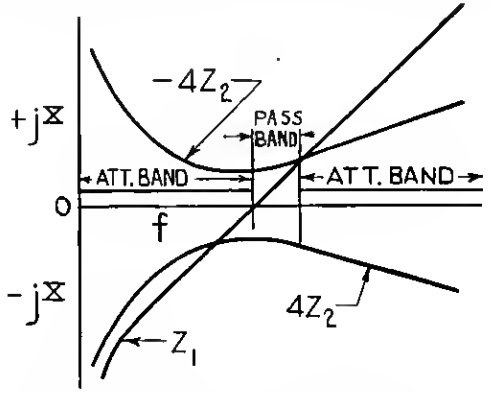

Fig. 46—Reactance-Frequency Characteristics of the Series and Shunt Arms of the Prototype Section of Fig. 45-A

$$f_1 = \frac{1}{2\pi\sqrt{L_1C_1}}. \tag{95}$$

Similarly, the upper cut-off frequency is that at which $Z_1 = -4Z_2$ or $j\omega L_1 - j/\omega C_1 = j4\omega L_2 + j4/\omega C_2$. From this relationship, the upper cut-off frequency is

$$f_2 = \frac{1}{2\pi}\sqrt{\frac{C_2+4C_1}{C_1C_2(L_1-4L_2)}}. \tag{96}$$

Let f_r be assumed as the frequency where Z_2 is a minimum, that is, where $\omega^2L_2C_2 = 1$. We may then write

$$f_r = \frac{1}{2\pi\sqrt{L_2C_2}}. \tag{97}$$

Substituting the above values of f_1, f_2 and f_r in formula (94) we obtain for $Z_1/4Z_2$

$$\frac{Z_1}{4Z_2} = \frac{1-\left(\frac{f}{f_1}\right)^2}{1+\left(\frac{f}{f_r}\right)^2} \cdot \frac{\left(\frac{f_2}{f_r}\right)^2+1}{\left(\frac{f_2}{f_1}\right)^2-1}. \tag{98}$$

From this last expression the attenuation and phase characteristics may be plotted from formulae (22) and (23) or from Figs. 11 and 12. The attenuation and phase constant characteristics are shown symbolically as characteristic 16 of Fig. 44. This structure has unusual attenuation properties which have already been discussed.

From equation (6) and the values of Z_1 and Z_2, in (92) and (93), the mid-series image impedance (Z_o), at the mid-frequency, is

$$Z_o = \frac{1}{2}\left[\sqrt{\frac{L_1}{C_1}+\frac{4L_1}{C_2}} - \sqrt{\frac{L_1}{C_2}-\frac{4L_2}{C_1}}\right]. \tag{99}$$

Since the mid-series image impedance, at any frequency, is the same as that of filter section 3—3, we have:

$$Z_I = Z_o\sqrt{1-\frac{\left[\frac{f}{f_m}-\frac{f_m}{f}\right]^2}{\left[\frac{f_2}{f_m}-\frac{f_m}{f_2}\right]^2}} = Z_o\sqrt{1-\frac{\left[\frac{1}{\sqrt{f_1f_2}}-\frac{\sqrt{f_1f_2}}{f}\right]^2}{\left[\sqrt{\frac{f_2}{f_1}}-\sqrt{\frac{f_1}{f_2}}\right]^2}} \tag{100}$$

where f_m is the mid-frequency ($f_m = \sqrt{f_1f_2}$), as before.

The prototype is not capable of mid-shunt termination, hence, its hypothetical mid-shunt impedance characteristic will not be derived.

From the preceding formulae, explicit expressions may be derived for the values of L_1, C_1, L_2 and C_2

$$L_1 = \frac{Z_o m'}{\pi(f_2-f_1)}, \tag{101}$$

$$C_1 = \frac{f_2-f_1}{4\pi f_1^2 Z_o m'}, \tag{102}$$

$$L_2 = \frac{-Z_o}{\pi(f_2-f_1)} \cdot \frac{1-m'^2}{4m'}, \tag{103}$$

$$C_2 = \frac{(f_2-f_1)m'}{\pi Z_o(f_2^2-f_1^2m'^2)}, \tag{104}$$

$$m' = \sqrt{1+\frac{\left(\frac{f_2}{f_1}\right)^2-1}{\left(\frac{f_r}{f_1}\right)^2+1}}. \tag{105}$$

As a numerical example of the solution of the prototype discussed assume, as in the example following equation (41), that the lower cut-off frequency f_1 is 20,000 cycles and that the upper cut-off frequency f_2 is 25,000 cycles. Assume f_r, a convenient parameter for the families of attenuation and phase constant curves which this section may have, for any given cut-off frequency, to be 30,000 cycles. Assume that the value of the mid-series image impedance Z_o at the mid-frequency is 600 ohms; then from formula (99) $m' = 1.083$: hence $L_1 = .0412$ henries, $C_1 = .00153 \times 10^{-6}$ farads, $L_2 = .00152$ henries and $C_2 = .0184 \times 10^{-6}$ farads. The structure with the numerical values of inductance and capacity for this specific example is shown in Fig. 47A.

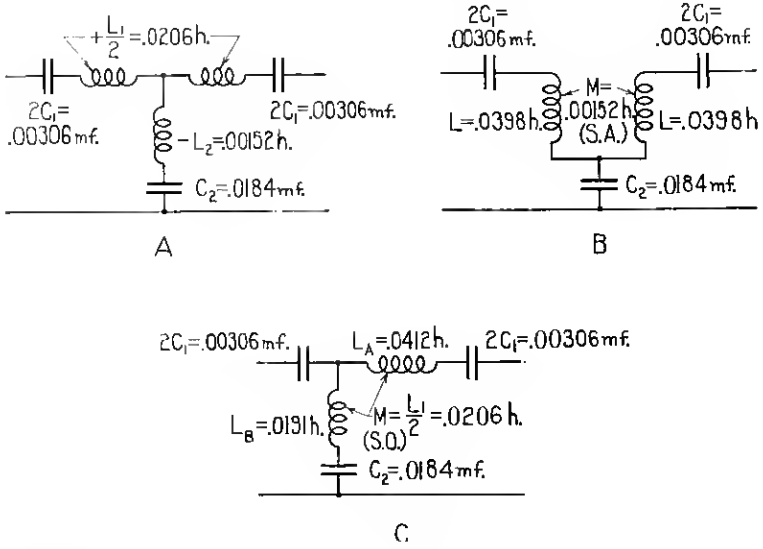

Fig. 47—Numerical Example of Equivalent Filter Sections Containing Negative Inductance

If, for the T mesh inductances in Fig. 47A, we substitute a transformer mesh having the values shown in Fig. 47 B, the mesh of the latter figure is electrically equivalent to the prototype structure and is an example of the method of employing the structure. Similarly, Fig. 47C illustrates the substitution of another type of three element mesh for the coil mesh of the prototype structure of Fig. 47A and is another example of the manner in which the prototype may be physically expressed.

The structure of Fig. 47B represents a similar case to that of 48A. However, as the mutual inductance is here series opposing, the proto-

type series-shunt equivalent structure is shown in Fig. 48B and contains no negative inductances. It will be found that the values chosen correspond to the numerical example of the structure 3—3 following equation 41.

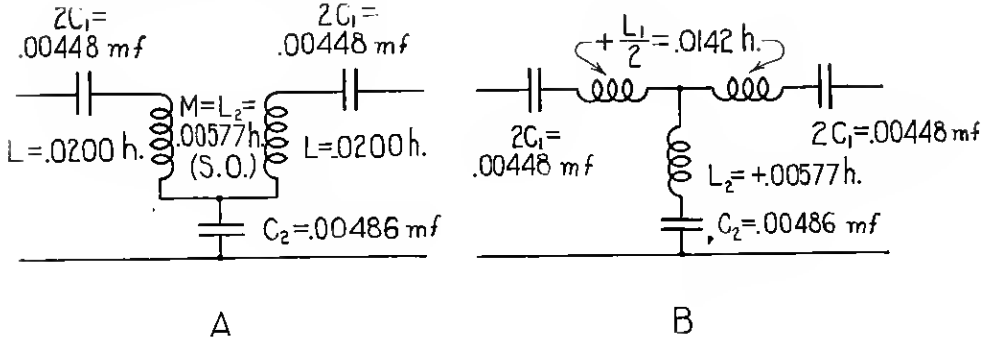

Fig. 48—Numerical Example of a Filter Section Containing No Negative Inductance

APPENDIX

Conditions for the Equality of the Image Impedances of Typical Filter Structures

It has been stated that the formation of recurrent and composite wave filters is dependent upon the maintenance of equal image impedance characteristics (of the sections or half-sections joined) at each junction point throughout the filter.

A general method of ascertaining the conditions for the equality of image impedance characteristics will be demonstrated by illustrations from typical pairs of sections.

Illustration No. 1—Negative Inductance in Shunt Arm of One Structure. Consider the filter sections listed as 3–4 (confluent structure) in Table II, and 3–1′ in Table III. It will be shown that, under proper conditions, their mid-series image impedance characteristics may be made equal at all frequencies. (By reference to the above tables, both sections have mid-series impedance characteristic No. 13 of Fig. 8).

From equation (6)

$$Z_I^2 = Z_1 Z_2 + \frac{Z_1^2}{4}. \tag{106}$$

In Fig. 49, let

$$Z_1 \equiv Z_{1A} + Z_{1B} = j\omega L_1 + \frac{1}{j\omega C_1}, \tag{107}$$

$$Z_1' \equiv K_A Z_{1A} + K_B Z_{1B}, \tag{108}$$

and $$Z_2' \equiv -K_C Z_{1A}, \tag{109}$$

where $K_A \equiv L_1'/L_1$, $K_B \equiv C_1/C_1'$ and $K_C \equiv L_2'/L_1$. (110)

From (106)

$$Z_I^2 = R^2 + \frac{Z_1^2}{4} \tag{111}$$

in which

$$R \equiv \sqrt{\frac{L_2}{C_1}} \equiv \sqrt{\frac{L_1}{C_2}}. \tag{112}$$

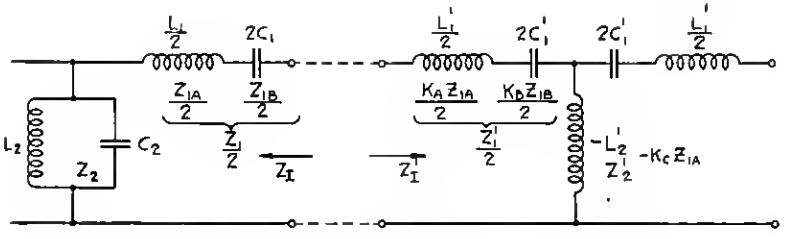

Fig. 49—Two Structures Having Equal Mid-Series Image Impedances, One of Which Contains a Negative Inductance in Its Shunt Arm

From (107) and (111)

$$Z_I^2 = R^2 + \tfrac{1}{4}(Z_{1A} + Z_{1B})^2 = 1/4Z_{1A}^2 + (1 + K/2)R^2 + 1/4Z_{1B}^2 \tag{113}$$

where $$K \equiv Z_{1A}Z_{1B}/R^2 = L_1/L_2 = C_2/C_1. \tag{114}$$

Now from (106) and (108)

$$(Z_I')^2 = Z_1'Z_2' + \frac{(Z_1')^2}{4} = \left(\frac{K_A^2}{4} - K_A K_C\right) Z_{1A}^2 + \left(\frac{K_A K_B}{2} - K_B K_C\right) K R^2 + \frac{K_B^2}{4} Z_{1B}^2. \tag{115}$$

Since, by postulation, in Fig. 49, $Z_1 = Z_1'$, we may equate the coefficients of (113) and (115). This gives

$$\frac{1}{4} = \frac{K_A^2}{4} - K_A K_C, \tag{116}$$

$$1 + \frac{K}{2} = \left(\frac{K_A K_B}{2} - K_B K_C\right) K, \tag{117}$$

and $$\frac{1}{4} = \frac{K_B^2}{4}. \tag{118}$$

Whence $$K_B \equiv \frac{C_1}{C_1'} = 1, \tag{119}$$

and $$K_A \equiv \frac{L_1'}{L_1} = \frac{L_1'C_1'}{L_1C_1} = \frac{f_M^2}{f_1^2} = \frac{f_2}{f_1}, \tag{120}$$

where f_1 and f_2 are the lower and upper cut-off frequencies, respectively, and $f_M \equiv \sqrt{f_1 f_2}$ of the structures of Fig. 49.

From (116) and (120)

$$K_C \equiv \frac{L_2'}{L_1} = \frac{1}{4}\left(K_A - \frac{1}{K_A}\right) = \frac{1}{4}\left(\frac{f_2}{f_1} - \frac{f_1}{f_2}\right). \tag{121}$$

Therefore, when the relationships between the constants of the two structures of Fig. 49 satisfy equations (119), (120) and (121), the structures will have the same mid-series image impedance characteristics. Explicit relations for the values of C_1', L_1' and L_2' may be obtained from equations (119), (120) and (121) as follows:

$$C_1' = C_1, \tag{122}$$

$$L_1' = L_1\frac{f_2}{f_1}, \tag{123}$$

$$L_2' = \frac{L_1}{4}\left(\frac{f_2}{f_1} - \frac{f_1}{f_2}\right). \tag{124}$$

Consequently, if the constants and cut-off frequencies of a confluent structure are known, the constants of a structure of the 3–1′ form having an identical mid-series image impedance characteristic can be derived from equations (122), (123) and (124).

Illustration No. 2—Negative Inductance in Series Arm of One Structure. Consider next the filter sections listed as 3–4 (confluent structure) in Table II and 1′–4 in Table III. It will be shown that, under proper conditions, their mid-shunt image impedance characteristics may be made equal at all frequencies. (By reference to the above tables, both sections have mid-shunt impedance characteristic No. 14 of Fig. 8).

From equation (7)

$$Y_I^2 = Y_1Y_2 + \frac{Y_2^2}{4}, \tag{125}$$

where $Y_1 = 1/Z_1$, $Y_2 = 1/Z_2$ and $Y_I = 1/Z_I$.

In Fig. 50, let

$$Y_2 \equiv Y_{2A} + Y_{2B} = \frac{1}{j\omega L_2} + j\omega C_2. \tag{126}$$

$$Y_2' \equiv K_A Y_{2A} + K_B Y_{2B}, \tag{127}$$

and

$$Y_1' \equiv -K_C Y_{2A}, \tag{128}$$

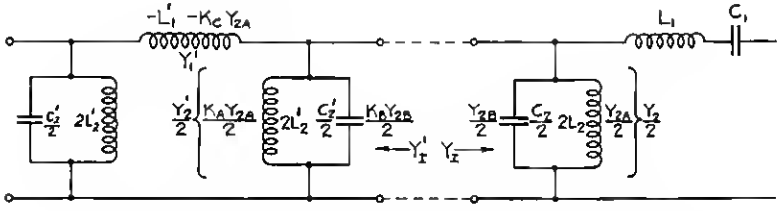

Fig. 50—Two Structures Having Equal Mid-Shunt Image Impedances, One of Which Contains a Negative Inductance in Its Series Arm

where $K_A \equiv L_2/L_2'$, $K_B \equiv C_2'/C_2$ and $K_C \equiv L_2/L_1'$. (129)

From (125)

$$Y_I^2 = G^2 + \frac{Y_2^2}{4} \tag{130}$$

in which

$$G \equiv \sqrt{\frac{C_1}{L_2}} \equiv \sqrt{\frac{C_2}{L_1}} \tag{131}$$

From (126) and (130)

$$Y_I^2 = G^2 + 1/4(Y_{2A} + Y_{2B})^2 = 1/4\, Y_{2A}^2 + (1 + K/2)G^2 + 1/4\, Y_{2B}^2 \tag{132}$$

where

$$K \equiv Y_{2A} Y_{2B}/G^2 = L_1/L_2 = C_2/C_1. \tag{133}$$

Now from (125) and (127)

$$(Y_I')^2 = Y_1' Y_2' + \frac{(Y_2')^2}{4} = \left(\frac{K_A^2}{4} - K_A K_C\right) Y_{2A}^2 +$$

$$\left(\frac{K_A K_B}{2} - K_B K_C\right) K G^2 + \frac{K_B^2}{4} Y_{2B}^2 \tag{134}$$

Since, by postulation, in Fig. 50, $Y_I = Y_I'$, we may equate the coefficients of (132) and (134). This gives

$$\frac{1}{4} = \frac{K_A^2}{4} - K_A K_C, \tag{135}$$

$$1 + \frac{K}{2} = \left(\frac{K_A K_B}{2} - K_B K_C\right) K, \tag{136}$$

and $$\frac{1}{4} = \frac{K_B^2}{4}. \tag{137}$$

Whence $$K_B \equiv \frac{C_2'}{C_2} = 1, \tag{138}$$

and $$K_A \equiv \frac{L_2}{L_2'} = \frac{L_2 C_2}{L_2' C_2'} = \frac{f_2^2}{f_M^2} = \frac{f_2}{f_1} \tag{139}$$

where f_1 and f_2 are the lower and upper cut-off frequencies, respectively, and f_M is the mean frequency $(\sqrt{f_1 f_2})$ of the structures of Fig. 50.

From (135) and (139)

$$K_C \equiv \frac{L_2}{L_1'} = \frac{1}{4}\left(K_A - \frac{1}{K_A}\right) = \frac{1}{4}\left(\frac{f_2}{f_1} - \frac{f_1}{f_2}\right). \tag{140}$$

Therefore, when the relationships between the constants of the two structures of Fig. 50 satisfy equations (138), (139) and (140), the structures will have the same mid-shunt image impedance characteristics. Explicit relations for the values of C_2', L_2' and L_1' may be obtained from equations (138), (139) and (140) as follows:

$$C_2' = C_2, \tag{141}$$

$$L_2' = L_2 \frac{f_1}{f_2}, \tag{142}$$

$$L_1' = \frac{4L_2}{\left(\frac{f_2}{f_1} - \frac{f_1}{f_2}\right)}. \tag{143}$$

Therefore, if the constants and cut-off frequencies of a confluent structure are known, the constants of a structure of the 1′—4 form having an identical mid-shunt image impedance characteristic can be derived from equations (141), (142) and (143).

BIBLIOGRAPHY

1. Thévenin, M. L., "Sur un Nouveau Théorème d'Electricité Dynamique," *Comptes Rendus*, Vol. 97, pp. 159–161 (1883).
2. Kennelly, A. E., "The Equivalence of Triangles and Three-Pointed Stars in Conducting Networks," *Electrical World and Engineer*, New York, Vol. XXXIV, pp. 413–414, Sept. 16, 1899.
3. Campbell, G. A., "Cisoidal Oscillations," *Trans. A. I. E. E.*, Vol. XXX, Part II, pp. 873–909 (1911).
4. Campbell, G. A., U. S. Patents Nos. 1,227,113 and 1,227,114 (1917).
5. Gherardi, B. and Jewett, F. B., "Telephone Repeaters," *Trans. A. I. E. E.*, 1919.
6. Wagner, K. W., *Arch. fur Elektrotechnik*, Vol. 8, p. 61 (1919); *E. T. Z.*, Aug. 7, 1919.

7. Van der Bijl, H. T., "Thermionic Vacuum Tubes," Published 1920.
8. Pierce, G. W., "Electric Oscillations and Electric Waves," Published, 1920.
9. Colpitts, E. H. and Blackwell, O. B., "Carrier Current Telephony and Telegraphy," *Trans. A. I. E. E.*, Feb., 1921.
10. Clement, L. M., Ryan, F. M., and Martin, D. K., "The Avalon-Los Angeles Radio Toll Circuit," *Proc. I. R. E.*, May, 1921.
11. Fletcher, H., "The Nature of Speech and Its Interpretation," *Jour. Franklin Inst.*, June, 1922.
12. Campbell, G. A., "Physical Theory of the Electric Wave-Filter," *Bell Sys. Tech. Jour.*, Nov., 1922.
13. Zobel, O. J., "Theory and Design of Uniform and Composite Electric Wave-Filters," *Bell Sys. Tech. Jour.*, Jan., 1923.
14. Rose, A. F., "Practical Application of Carrier Telephone and Telegraph in the Bell System," *Bell Sys. Tech. Jour.*, April, 1923.
15. Hartley, R. V. L., "Relation of Carrier and Side-Bands in Radio Transmission," *Bell Sys. Tech. Jour.*, April, 1923.
16. Bown, C. D., Englund, C. R., and Friis, H. T., "Radio Transmission Measurements," *Proc. I. R. E.*, April, 1923.
17. Peters, L. J., "Theory of Electric Wave Filters Built up of Coupled Circuit Elements," *Jour. A. I. E. E.*, May, 1923.
18. Demarest, C. S., "Telephone Equipment for Long Cable Circuits," *Bell Sys. Tech. Jour.*, July, 1923.
19. Nichols, H. W. and Espenschied, L., "Radio Extension of the Telephone System to Ships at Sea," *Bell Sys. Tech. Jour.*, July, 1923.
20. Carson, J. R. and Zobel, O. J., "Transient Oscillations in Electric Wave-Filters," *Bell Sys. Tech. Jour.*, July, 1923.
21. Arnold, H. D. and Espenschied, L., "Transatlantic Radio Telephony," *Bell Sys. Tech. Jour.*, Oct., 1923.
22. Best, F. H., "Measuring Methods for Maintaining the Transmission Efficiency of Telephone Circuits," *Jour. A. I. E. E.*, Feb., 1924.
23. Casper, W. L., "Telephone Transformers," *Jour. A. I. E. E.*, March, 1924.
24. Slaughter, N. H. and Wolfe, W. V., "Carrier Telephony on Power Lines," *Jour. A. I. E .E.*, April, 1924.
25. Foster, R. M., "A Reactance Theorem," *Bell Sys. Tech. Jour.*, April, 1924.
26. Martin, W. H., "The Transmission Unit and Telephone Transmission Reference System," *Bell Sys. Tech. Jour.*, July, 1924.
27. Zobel, O. J., "Transmission Characteristics of Electric Wave-Filters," *Bell Sys. Tech. Jour.*, Oct., 1924.